AD-775 231

CREEP FRACTURE OF ROCK

Wolfgang R. Wawersik, et al

Utah University

Prepared for:

Advanced Research Projects Agency

July 1973

14. KEY WORDS	LINK A		LINK B		LINK C	
	ROLE	WT	ROLE	WT	ROLE	WT
Rock						
granite						
sandstone						
marble						
strain measurement						
shear stress						
confining pressure						
complete quasi-static stress strain curves						
creep						
creep fracture						
constitutive equations						

AD-775231

Unclassified

Security Classification

3200.8 (Att 1 to Encl 1)
Mar 7, 66

DOCUMENT CONTROL DATA - R & D

(Security classification of title, body of abstract and indexing annotation must be entered when the overall report is classified)

1. ORIGINATING ACTIVITY (Corporate author)

University of Utah, Salt Lake City, Utah 84112

2a. REPORT SECURITY CLASSIFICATION

Unclassified

2b. GROUP

3. REPORT TITLE

"Creep Fracture of Rock"

4. DESCRIPTIVE NOTES (Type of report and inclusive dates)

Final Report December 28, 1971 - July 8, 1973)

5. AUTHOR(S) (First name, middle initial, last name)

Wolfgang R. Wawersik and Wayne S. Brown

6. REPORT DATE

July 1973

7a. TOTAL NO. OF PAGES

84

7b. NO. OF REFS

75

8a. CONTRACT OR GRANT NO.

H0220007

b. PROJECT NO.

1579

c.

d. Program Code No. 2F10

9a. ORIGINATOR'S REPORT NUMBER(S)

9b. OTHER REPORT NO(S) (Any other numbers that may be assigned this report)

10. DISTRIBUTION STATEMENT

Distribution of the document is unlimited

11. SUPPLEMENTARY NOTES

12. SPONSORING MILITARY ACTIVITY

Advanced Research Projects Agency

13. ABSTRACT

Experiments were conducted to assess the time-dependent behavior of brittle rock and of rough, unfilled tension joints as a function of stress state and water content at ambient temperature. Quasi-static tests were performed on Westerly granite, Nugget sandstone and Tennessee marble at confining pressures up to 10,000 psi. Creep was measured on granite and sandstone at 1,000 psi, 5,000 psi and 10,000 psi confining pressure. Finally, creep tests were carried out on granite in uniaxial tension. Both axial and lateral strains ε_1 and $\varepsilon_3 \approx \varepsilon_2$ were measured in all experiments.

All results indicate the creep in rock at high stress is a complex phenomenon which is non-linearly related to stress and which is not adequately modelled by any known creep law. Fortunately, from a practical point of view, creep and creep fracture in competent or jointed rock are deemed significant only in the immediate vicinity of underground structures. Hence for the type of rocks studied it is anticipated the stability of underground excavations and of the artificial support systems of such excavations will not deteriorate markedly with time unless adverse pore pressures are encountered.

DD FORM 1 NOV 1473

Security Classification

ARPA Order Number:
1579

Program Code Number:
2F10

Name of Contractor:
University of Utan

Effective Date of Contract:
December 28, 1971

Contract Expiration Date:
February 28, 1973

Amount of Contract:
$29,997

Contract Number:
H0220007

Principal Investigators and Phone Number:
W. R. Wawersik
W. S. Brown 801-581-6441

Project Scientists or Engineers and Phone Number:
Same

Short Title of Work:
Creep Fracture of Rock

FINAL REPORT

Sponsored by
Advanced Research Projects Agency
ARPA Order No. 1579, Program Code 2F10

July 1973

ACKNOWLEDGEMENTS

This research was supported by the Advanced Research Project Agency of the Department of Defense and was monitored by Mr. Peter G. Chamberlain of the Twin Cities Mining Research Center, U. S. Bureau of Mines under Contract No. H022007. Funds for the design and fabrication of a new differential pressure gauge were generously provided by Dr. Samuel S. Kistler, Professor Emeritus, University of Utah.

We thank Mr. Peter Chamberlain for several helpful discussions and suggestions during the course of this study. Special appreciation is extended to Mr. Richard Thill of the U. S. Bureau of Mines, Twin Cities Research Center. Mr. Thill conducted all ultrasonic velocity measurements which are referred to in this report. We also thank Professor W. F. Brace Massachusetts Institute of Technology for several helpful discussions concerning the design of high pressure equipment. Messrs. Craig Cooley, Richard Dropek and Carl Brechtel participated in the assembly of equipment, performance of experiments and in the reduction of experimental data. Finally, we acknowledge the help and outstanding workmanship of Messrs. Dieter Steinmann, Hans Seurig and Howard Spencer, machinists and technicians in the Department of Mechanical Engineering, University of Utah.

TABLE OF CONTENTS

TECHNICAL REPORT SUMMARY

Quasi-static loading experiments and creep tests were conducted under confining pressure, in uniaxial compression and in uniaxial tension. Quasi-static tests were performed on Westerly granite, Nugget sandstone, and Tennessee marble at confining pressures up to 10,000 psi. Creep was measured on granite and Nugget sandstone in uniaxial compression and at 1,000 psi, 5,000 psi, and 10,000 psi confining pressure. Finally, creep tests were carried out on Westerly granite in uniaxial tension. Both axial and lateral strains, ε_1 and $\varepsilon_2 \approx \varepsilon_3$, were measured in all experiments. The results obtained may be summarized as follows:

1. Regardless of the state of stress, creep in granite was characterized by the three stages of primary, secondary and tertiary creep. In compression, creep accelerated gradually during tertiary creep providing some warning that creep fracture was impending. In uniaxial tension the tertiary creep was of very short duration. Consequently, creep fracture of granite subjected to uniaxial tension was sudden irrespective of the magnitude of the secondary creep rate.
2. Creep in granite was non-linearly related to stress. In all compression tests a strong coupling was observed between shear strains and volumetric strains, i.e. both strain components were functions of the shear stress and the mean stress. Creep in Nugget sandstone was further complicated by the fact that it was governed by competing mechanisms, probably time-dependent compaction (pore collapse) and micro-cracking. If generally true these results obviously invalidate most if not all existing time-dependent constitutive equations for rock including the set of emperical formulae

which were proposed in an earlier study, "Creep Fracture of Rock in Uniaxial Compression", to describe the time-dependent behavior of granite and sandstone in uniaxial compression.

3. In the ranges of shear stress and confining pressure which were explored in creep tests on granite the shear strains and the volumetric strains always were of the same order of magnitude. This fact has not been incorporated into any published creep law.
4. Shear-strains and volumetric strains during creep in granite increased rapidly with increases in the shear stress; they decreased as the confining pressure was raised.
5. Although no tests were carried out at elevated pore pressure it is suspected that creep is related to the magnitude of the effective stresses, i.e. applied stresses minus pore pressure. It is anticipated, therefore, that time-dependent deformations in rock will be influenced by changes in pore pressure regardless of the nature of the pore fluid.
6. Creep and creep fracture observations on granite indicate that the times-to-failure at fixed shear stresses will increase by orders of magnitude with increasing confining pressure. Hence creep fracture is much less likely to occur under confining pressure than it is in uniaxial compression. This suggestion is partly based on measured changes of the secondary creep rates as a function of confining pressure. In part it is also inferred from increases in the limiting creep strains which were estimated by means of published complete quasi-static stress-strain data for air-dry Westerly granite.
7. Time-dependent deformations in granite and sandstone were augmented by increases in water content. In uniaxial compression the secondary

creep rates in air-dry and water-saturated specimens were found to differ by approximately two orders of magnitude. Comparisons of the quasi-static behavior of both rocks indicate that the effect of water might be equally pronounced at elevated confining pressure. Finally,

8. A few measurements on granite samples containing artificially created tension joints suggest that creep on rough, unfilled joints is negligibly small. The coefficient of friction on such joints was found to increase with the time that the joint surfaces were subjected to constant normal and shear stresses. These observations corroborate results which were recently published by Dietrich (16).

For the rocks tested in this investigation the practical consequences of all results are relatively reassuring. Time-dependent deformation and failure of competent rock are considered potentially hazardious only in tension and in compression at high shear stress and low confining pressure (mean stress), i.e. in the immediate vicinity of underground excavations. Their importance is anticipated to decrease rapidly with distance away from such openings unless the effective confining confinement of the rock is lessened by pore pressure. As a result it is deemed unlikely that large time-dependent deformations and associated load changes on support systems will occur. If it is assumed that the mechanical behavior of rock masses typically is controlled by the properties of joints, then it is further suggested that time-dependent effects become insignificant unless time and water sensitive filling materials are encountered. In the absence of such materials the stability of jointed rock appears to be governed solely by its instantaneous response to changes in stress state.

LIST OF FIGURES

INTRODUCTION

Time-dependent rock deformation and failure are phenomena which are poorly understood. Their practical significance is evidenced in such situations as closure of mine openings, movements in foundations, or fault motions, etc. However, there is neither hard evidence to show that time is a contributing factor nor are there proven time-dependent constitutive relations which would permit long-term ground motions to be predicted. To deal with existing uncertainties concerning the influence of time, a comprehensive research project was initiated. In its first phase, this work was concerned with time-dependent rock deformation and failure in uniaxial compression. Based on reports that the presence of water will accentuate the time sensitivity of rock, air-dry and water-saturated specimens were tested in quasi-static loading experiments and creep tests. The results of this study were presented in an earlier report entitled, "Creep Fracture of Rock in Uniaxial Compression" (1). The data for three rock types, (Westerly granite, Nugget sandstone and Tennessee marble), indicated that creep and time-dependent failure are significant in rocks exhibiting Class II failure behavior. The presence of water was found to increase creep quite markedly, and after 1,000 hours, the strength of water-saturated specimens was observed to decrease to approximately 50 per cent of the quasi-static compressive strength in the air-dry condition.

To predict creep and creep fracture in uniaxial compression, a set of emperical, non-linear, time-dependent stress-strain equations were formulated and a scheme was proposed to determine the fracture time of rock. This scheme was based on the observation that stable creep strains in uniaxial compression parallel to the loading direction are bounded by the post-failure strains of complete stress-strains curves which are established in quasi-static experi-

ments at strain rates of approximately 10^{-5}/sec.

While satisfactory agreement was achieved between prediction and experiment in uniaxial compression, the work conducted during the first phase of this project had two obvious shortcomings: (1) It was restricted to uniaxial compressive loading and (2) only one principal strain component was measured. Consequently, the conclusions derived from these earlier tests are difficult to generalize and leave several important questions unanswered: What is the effect of the mean stress? How do volume and shear strain vary with stress? How can the influence of water on the time-dependent behavior of rock be described? Is it the same under confining pressure as it is in uniaxial compression? What happens when one principal stress is tensile?

With these questions in mind, further exploratory experiments were developed under confining pressure and in uniaxial tension. In addition, tests were initiated on unfilled joints (artifically introduced tension fractures) to ascertain the time-dependent properties of weakness planes which are believed to dominate the mechanical response of rock masses. Particular efforts were made throughout this study to monitor all principal strain components and, therefore, to provide data which would permit meaningful mathematical models to be developed if they are needed.

Several short-cuts had to be taken to complete this research in spite of the large variety of experiments and in spite of the limited amount of funds and time available. First, the number of experiments in each category had to be kept small. Secondly, tests were not conducted consistently on either or both air-dry and water-saturated rock. This was necessary because some of the standard experimental techniques used failed in the presence of water and because the development of new experimental methods had to be held to a minimum. For these reasons, for example, only air-dry samples were tested in uniaxial tension.

To attain a better understanding about the influence of water, earlier experiments were supplemented by tests on air-dry samples in uniaxial compression. The results of these tests and data from new quasi-static experiments also furnished a basis for the qualitative comparison of the behavior of air-dry and water-saturated specimens under confining pressure.

Thus, the second year effort, "Creep Fracture of Rock", is concerned with time-dependent deformation and failure of rock under a broad spectrum of stress states. Complete sets of strain measurements were made and efforts were undertaken to describe the influence of water in quasi-static and creep experiments. Accordingly, this research was divided into four tasks:

1. Quasi-static and creep tests on water saturated rock under confining pressure
2. Creep experiments on air dry rock in uniaxial compression
3. Quasi-static and creep tests in uniaxial tension
4. Quasi-static and creep tests on jointed rock specimens

Finally, attempts were undertaken to delineate the damage to the rock fabric in creep with the hope that such observations would suggest methods by which impending time-dependent rock fracture might be predicted in-situ.

LITERATURE REVIEW

An extensive discussion of past work on the time-dependent deformation and failure of rock was provided in the earlier report entitled, "Creep Fracture of Rock in Uniaxial Compression" (1). For the sake of completeness the reference list which was compiled then is included in this report as an appendix.

Most published research into the time-dependent properties of rock has focused on the development of suitable stress-strain relations which include the influence of temperature (1). These equations are mainly based on measurements of only one strain component and are limited to either uniaxial compression or tension (1-5, 19). The majority of equations appears to be valid for constant stress rather than time-varying stress conditions and all of them pertain to competent rock. Only very few experiments provide any clues concerning the time-dependent behavior of rock under confining pressure. Among these are the well known experiments of Griggs, Heard, Serdengecti and Boozer, Le Comte and most recently of Goetze and Rutter (19, 1, 3, 6, 7). The results of these tests suggest that time-dependent effects might become less prevalent under confining pressure than under unidirectional loads. However, no definite conclusions can be drawn to date because most of these confining pressure experiments concentrated on the influence of temperature rather than pressure. Some of them were carried out at strain rates exceeding 10^{-3}/sec. so that extrapolations into the regime of long term creep might be questionable.

Time-dependent fracture and the influence of water concentrations were studied recently by Swolfs (8), Martin (19), McCarter and Willson (9), and Scholz (10) using sandstones or single-crystal quartz. The results of these and earlier tests (Appendix) have established that time-dependent

(delayed) fracture can be significant, especially in the presence of water. They have also demonstrated that time-dependent fracture in rock, particularly in silicate rocks, is due to progressive micro-fracturing and thus might be predicted from the history of the micro-seismic activity prior to fracture. This approach was taken successfully to forecast a major slope failure in an open pit mine in Chile (11).

Many of the results mentioned above were corroborated by observations which were made during the first year of this study (1) as well as by Haimson et al (12, 13) and by Peng and Podnieks (14). It is emphasized, however, that all of these data were obtained in uniaxial loading experiments. Hence predictions of similar effects under confining pressure are speculative.

Since the inception of the research which is summarized in this report, at least two investigators, Handin et al. (15) and Dietrich (16) have published results on the time-dependent behavior of joints. Specifically they have considered the relationship between time and the coefficients of sliding friction and stress drops past the onset of slip. In general, the coefficients of friction of joints were found to remain constant or to increase with loading duration depending on the roughness of the joint surfaces and on the amount of accumulated gouge. Stress drops during unstable sliding on effectively smooth joint surfaces or on filled joints became greater as well. Thus, for the type of joints which were studied by Handin et al. and by Dietrich, it appears that the long-term ultimate strength of joints might actually exceed the short-term strength.

ROCK TYPES AND SPECIMENS

Three rock types were used for the various tasks of this investigation: Westerly granite, Nugget (Navajo) sandstone and Tennessee marble. All three had previously been tested in uniaxial compression under quasi-static and constant loading conditions. Some basic rock properties are listed in Table I.

Cylindrical samples one inch in diameter and approximately 2.3 inch in length were tested. Every specimen of each rock type was drilled in one direction out of the same block. For Nugget sandstone, specifically, the bedding planes lay perpendicular to the sample axes. All specimen surfaces were ground prior to testing. The specimen ends were machined parallel to within 0.0002 inch.

Both air-dry and water-saturated samples were used. Air-dryness was achieved by exposing each specimen to room conditions at relatively constant humidity ratios (0.0045 to 0.005) and temperature (73^{o}F). The procedure for water saturation is described in Reference 1.

Cylindrical "jointed" specimens were obtained by inducing tension fractures between line loads in rectangular blocks, gluing the fracture surfaces and subsequently drilling cores. The freshly cored specimens were then cut and ground to length and immersed into a solvent to remove all epoxy. All joint planes were oriented at a 30^{o} angle from the sample axes. The peak amplitudes of asperities along the joints were approximatley $\pm$ 0.020 in.

Rock Type	Grain Size (mm)	Porosity (%)	Major Constitments
Westerly granite	0.75	0.9	mica, quartz, and anarthosite (ref A53)
Nugget (Navajo sandstone)	larger mode 0.135 smaller mode 0.07	7	quartz
Tennessee marble	2.3	0.4	calcite

TABLE I. Rock Properties

DESCRIPTION OF EXPERIMENTS

Scope of Experiments

Time-dependent rock behavior was evaluated in creep and creep fracture experiments under confining pressure, in uniaxial compression and in uniaxial tension. One loading system was available for each part of the experiment.

Creep tests on rock are known to be time consuming and plagued by considerable data scatter. Therefore, it was impossible to study each of the three rock types considered and to conduct an arbitrary number of experiments. Instead, one rock, Westerly granite was singled out for a more detailed investigation and tests were limited to stress levels above which the possibility of creep fracture existed. Both the selection of granite and the choice of the stress range in which creep was to be studied was based on the results of quasi-static experiments at a strain rate of order 10^{-5} sec^{-1}. In uniaxial tension these tests were performed on air-dry specimens only. In all compression tests the behavior of air-dry and water-saturated samples was compared. In subsequent creep tests under confining pressure only water-saturated specimens were used in which creep appeared to proceed most rapidly and which, therefore, permitted a maximum number of data to be collected in the time available

Loading Apparatus

Uniaxial Compression

All uniaxial compression tests were carried out in one 50 kip hydraulic loading machine. During the creep experiments, the load was held constant by means of a set of gas accumulators which were placed in series with the actuator. Details of the equipment are described in Reference 1.

Confining Pressure

Axial load was generated by means of a 115 kip actuator in a standard

loading frame. Confining pressure was applied in the pressure vessel depicted in Figure 1(a)). It accommodates samples one inch in diameter by 2 3/4 inch long. The samples were loaded between two pistons of identical diameter and jacketed in loosely fitting polyurethane membranes. To test water-saturated specimens at reasonably constant (atmospheric) pore pressure, all samples were vented through small holes in the loading pistons.

Pressure was applied by means of a hand pump and/or by means of a screw-driven pressure regulator (Figure 1(b)). The design of the pressure regulator is based on a similar design by W. F. Brace. To maintain constant pressure in long-term creep experiments, the action of the pressure regulator was servo-controlled (Figure 1(b)) using the output of a specially fabricated differential pressure gauge (Figure 1(c)) as the feedback signal. A schematic of the entire confining pressure system is included as Figure 2.

The loading and pressure control procedure was effected as follows. As the confining pressure was applied in the beginning of an experiment, both ports of the differential pressure gauge were open. After the confining pressure had reached and stabilized a a pre-determined value, one side of the differential pressure gauge was isolated by means of a valve (Figure 2). The pressure of the fluid entrapped in the isolated reference side of the differential pressure gauge then provided a reference pressure which was maintained in the pressure vessel (active) side through the action of the pressure regulator.

The key to the operation of the confining pressure system was the successful design of a new differential pressure gauge (Figure 1(d)). This gauge had to meet three requirements: (1) It had to withstand line pressures of at least 15,000 psi; (2) its resolution had to be better than $\pm$ 5 psi, and (3) its overload range had to be no less than $\pm$ 3,000 psi. The high

overload capability was necessary to avoid any damage to the instrument as a result of pressure surges during uncontrolled brittle rock fracture. The adopted design employes a bellows and a Linear Variable Differential Transformer (LVDT) as sensing elements.

Uniaxial Tension

The tension apparatus consists of a double acting hydraulic cylinder, Spherco rod-end bearings and a ring-shaped load cell (Figure 1(d)). Each sample was epoxied to the two cylindrical end pieces. The end pieces were then connected to the fixed and movable crossheads of the testing machine by means of a short, threaded stud. Two accumulators which were placed in series with the actuator served to apply load in quasi-static tests or to maintain a constant load in creep experiments.

Specimen alignment proved to be a major problem. The strain distribution in our specimens was never uniform in spite of accurate sample machining, alignment of end-caps and rock samples, and several other measures. In general, the axial strain which was measured at three points spaced at 120^{o} around the circumference and midway between the specimen ends differed by as much as 14 per cent from the smallest observed reading.

Force and Strain Measurement on Competent Rock

Force was monitored simultaneously by means of strain gauge instrumented load cells and with a temperature compensated Heise pressure gauge. The Heise pressure gauge which measured the pressure in the hydraulic actuators was utilized mainly in long term creep experiments exceeding 24 hours.

Axial strain was measured either indirectly by monitoring end-to-end sample displacements (compression tests) or directly by means of SR 4 strain gauges (tension experiments). In uniaxial compression and in tension, the lateral on tangential strain was ascertained with the aid of SR 4 strain gauges.

In confining pressure tests, the lateral (radial) strain was determined from measurements of the integrated radial sample deformation. This technique was first employed by Crouch (17). It is based on the fact that the volume adjustments of the confining pressure medium which are needed to maintain a fixed confining pressure during radial sample deformation are directly proportional to the (average) radial specimen strain. Thus, for homogeneous specimen deformation it can be shown that:

$$\varepsilon_3 = \varepsilon_2 = \frac{1}{1 - \varepsilon_1} \left[\frac{\Sigma \Delta V}{C_1} - (C_2 \varepsilon_1 + C_3) F + (A_R - A_s) \frac{F}{K C_1} \right] \qquad (1)$$

where

$$C_1 = 2 A_R L_R$$

$$C_2 = \frac{\nu_s}{E_s A_R}$$

$$C_3 = C_2 \left(\frac{L_p - L_R}{L_R} \right)$$

$$K = \frac{K_R K_s}{K_R + K_s} \; ; \; K_R = \frac{E_R A_R}{L_R} \; ; \quad K_s = \frac{E_s A_s}{L_p - L_R}$$

The symbols in Equation (1) denote the following:

E_R = tangent (Young's) modulus of test specimen

A_R = cross sectional area of test sample

L_R = length of test sample

E_s, ν_s = elastic constants of loading piston material

A_s = cross sectional area of loading pistons

L_p = effective internal length of pressure vessel

F = axial force, and

$\Sigma \Delta V$ = cumulative, incremental volume adjustments of confining pressure medium

According to Equation (1) the radial sample strain can be monitored if it is possible to determine the volume adjustments of the confining pressure medium. In our system this was accomplished simply by tracking the motion of the servo-controlled i.e. automatically adjusted pressure regulator.

In this investigation the diameters of rock specimens and loading pistons were matched ($A_R = A_s$) and the strains encountered were small. Under these conditions Equation (1) can be reduced to:

$$\varepsilon_2 = \varepsilon_3 = \frac{\Sigma \Delta V}{C_1} - C_3 F \qquad (2)$$

To verify the validity of Equations (1) and (2), four calibration tests were conducted on standard samples of aluminum, brass, and steel of known elastic constants. These tests served to substantiate that $C_1 = 2A_R L_R$, to determine the constant C_2 and to ascertain the effective value of L_p which includes the unpredictable influence of all O-ring seals. An additional six calibration tests were carried out on standard samples of various lengths and diameters.

The worst discrepancy among measured physical properties determined indirectly as described above and directly by means of direct-bond strain gauges was 1.8 per cent of the smallest observed reading. Generally data using both techniques agreed to within better than 1 per cent. The Poisson's ratio of mild steel in the plastic range was determined only indirectly as 0.50 after strain gauges began to "peel" and render spurious, excessively large readings.

Obviously, the scheme of radial strain measurement provided by Equation (1) is valid only if the confining pressure systems is leak proof. To test this, a hardened steel specimen was jacketed and subjected to constant axial load and confining pressure for six days at the beginning and at the very end

of this study. No net change in pressure was observed. Small, temperature induced pressure variations were equal in the active and in the reference sides of the differential pressure gauge and, therefore, rendered no false readings.

Crouch (17) alluded to the accuracy of the above indirect technique for monitoring radial strains in confining pressure experiments. Combined with a servo-system the technique is also very economical. The savings in set-up time and strain gauges is estimated to be $30 per test. The method is particularly useful where strain gauges cannot be employed, for example on wet specimens or when large strains are encountered.

Deformation Measurements on Joints

Characterizations of the deformation of joints require that the relationships between the average normal stress, σ_n, and the average shear stress, τ_n, on the joint on one hand and the average normal and shear displacements, d_n and d_s, on the other be measured. If the rock containing the joint is homogeneous, i.e. if stress-strain data for competent samples are reproducible, then the displacements d_n and d_s associated with the joint can be calculated from comparative measurement of average axial and volumetric strains of competent and jointed samples. To demonstrate this point, in Figure 3 shear stress is plotted versus strain. Strain here denotes either volume strain or axial strain. Clearly, the difference in strain between the competent and the jointed sample $\Delta\varepsilon$ at any stress level must be due to the joint. From this difference the average normal deformation on a single joint is calculated as

$$d_n = \frac{V_R}{A_j} \Delta\varepsilon \qquad (3)$$

where

V_R = sample volume, and

A_j = joint area

$\Delta\varepsilon$ = difference in volumetric strain between competent and jointed specimen

Once d_n is known, the average joint shear displacement d_s is given by the relationship

$$d_s = \frac{\Delta\varepsilon_1 L_R - d_n \sin\alpha}{\cos\alpha} \tag{4}$$

where

L_R = specimen length

α = (smallest) angle between slip direction and specimen axis

$\Delta\varepsilon_1$ = difference in axial strain between competent and jointed specimen

EXPERIMENTAL RESULTS

Quasi-Static Compression Tests Under Confining Pressure

All relevant data obtained in 42 experiments are summarized in Table II. Figure 4 shows a typical original record of force versus axial and radial strain (displacement) for air-dry Tennessee marble subjected to 1,000 psi confining pressure. Figures 5 and 7 depict typical stress-strain curves for Westerly granite and Nugget sandstone. Figure 6 presents graphs of stress difference $\sigma_1 - \sigma_3$ versus volumetric strain ε and shear strain $\gamma = \varepsilon_1 - \varepsilon_3$

Complete stress-strain curves could be obtained only at 1,000 psi confining pressure. This is partly due to the low stiffness of our testing machine. Mainly this is attributed to the fact that the axial stress-strain response which is crucial for manual fracture control was always masked by the deformation of the loading pistons. The effect of the loading pistons can be taken into account in subsequent data reductions but not instantaneously while an experiment is in progress.

The lack of complete stress-strain curves at confining pressures above 1,000 psi severely hampered the study of time-dependent rock fracture. According to a scheme described earlier (1) time-dependent rock fracture in creep might be predicted once the total creep strain ε_c prior to the onset of accelerated creep is known. The results of uniaxial compression experiments indicated that an upper bound of the quantity ε_c in turn can be estimated from complete stress-strain curves as the difference in strain-between the ascending and descending branches of these curves at any given stress level. In the absence of such complete stress-strain curves such bounds could not be established reliably.

Rock Type	Confining Pressure $\sigma_2 = \sigma_3$ (10^3 psi)	Ultimate Strength $\sigma_1-\sigma_3$, (10^3 psi)		Estimated Onset of Micro-cracking $C = \sigma_1 - \sigma_3$, (10^3 psi)	
		Air-Dry	Water-Saturated	Air-Dry	Water-Saturated
Westerly granite	0	37.4 (±3.7%)	33.2	18.8	18.2
	1	49.8 (±2.9%)	43.7	?	22.5
	5	80.5 (±1.3%)	72.6	?	34.8
	10	111.5 (±1.2%)	105.5	?	48.8
Nuggett Sandstone	0	33.4 (-5.4% + 6.7%)	29.4	?	?
	1	38.6 (-8.9% + 8.5%)	35.1	?	?
	5	66.5 (-4.6% + 7.0%)	61.2	?	?
Tennessee Marble	0	16.2 (±3.6%)	15.5	?	?
	1	20.3 (±3.0%)	19.5	?	?
	5	30.0	28.8	?	?

TABLE II. Rock Properties for Westerly Granite, Nugget Sandstone, and Tennessee Marble under Quasi-Static Loading Conditions; Strain Rate $0(10^{-5})sec^{-1}$.

At all pressures Tennessee marble sustained by far the largest strain before a loss in loading bearing ability occurred. Its post-failure behavior is clearly of type Class I (19). Thus, time-dependent failure of marble was judged unlikely in comparison with granite and sandstone (1). Also, Tennessee marble appeared to be the least sensitive to the presence of water (Table II).

Both granite and sandstone exhibited very brittle behavior. Complete stress-strain curves obtained here at 1,000 psi confining pressure show that the loops between the ascending and descending branches of the curves are narrow compared with Tennessee marble and, therefore, that time-dependent fracture in creep might occur within relatively short time spans.

The influence of water on the ultimate stress (peak stress) was approximately equal in granite and sandstone. The ultimate stress of water-saturated samples of both rocks was 10 per cent to 13 per cent lower than their strengths in the air-dry state. This decrease in ultimate stress at the same externally imposed strain rate of $O(10^{-5})$/sec. indicates that time-dependent effects become more pronounced in the presence of water.

It is noticeable that the granite data are more reproducible than the results for sandstone. This observation above all governed the choice of Westerly granite as the principal test rock in subsequent creep experiments.

The shear stress, C for which micro-cracking is proported to commence, was determined for Westerly granite (Table II). The shear-stress C was defined as the stress intercept of two straight lines drawn tangent to curves of principal stress difference versus volume strain (Figure 6). One line was drawn tangent to the approximately linear portion of the curve below one half the ultimate stress; the other was drawn vertical through the point of maximum volume compression (Figure 6). The value of C used here could be more readily defined from the available experimental records than the true value which characterizes the first departure of the curves mean stress versus volume strain from the hydrostat.

Creep Experiments Under Confining Pressure

Fifteen creep experiments were conducted on water-saturated Westerly granite under confining pressures of 1,000 psi, 5,000 psi and 10,000 psi. All specimens were loaded axially at a strain rate of approximately 10^{-5}/sec. from a state of hydrostatic compression to the predetermined (constant) creep load. This low strain (loading) rate provided some assurance that no significant pore pressure would be generated due to slow drainage. The duration of individual creep experiments varied between six hours and 500 hours.

A set of typical creep curves of ε_1 and ε_3 versus time are presented in Figures 8 and 9 for two specimens subjected to 5,000 psi confining pressure and stress differences of 64,600 psi and 64,900 psi times the mean ultimate strength in quasi-static compression. The data shown are representative both for the regularity of individual sets of data and for the variability of the results between tests. Throughout it was assumed that $\varepsilon_3 = \varepsilon_2$ because the radial deformation of all rock cylinders was approximately homogeneous.

Given enough time, creep in ε_1 and ε_3 is characterized by the well known stages of primary (transient) secondary ("steady state") and teriary creep (Figure 8). However, tertiary creep and terminal creep fracture were observed in only four experiments.

Primary creep, ε_{1II} and $\varepsilon_{3I} \approx \varepsilon_{2I}$, was most readily described by a power function of time:

$$\varepsilon_{iI} = 10^{C_i} t^{n_i} \qquad (5)$$

Approximate values of C and n were determined from double logarithmic plots of strain versus time. Values which describe the axial strain ε_{1I} parallel to the greatest applied compression are contained in Table III and in Figure 10. However, there is some evidence that the observed primary creep

$\sigma_2 = \sigma_3$ 10^2 psi	σ_1 10^3 psi	$\varepsilon_{1I} \simeq 10^{C_1} t_1$	
		C_1+6	n_1
0	25.0	1.5	0.39 (0.11)
0	30	2.3	0.39 (0.30)
0	31	2.5	0.39 (0.38)
0	33	3.0	0.39 (0.41)
1	32.4	2.6	0.41
1	33.0	2.1	0.32
1	36.3	2.28	0.25
1	40.2	1.63	0.21
5	58.8	2.32	0.11
5	62.7	2.02	0.25
5	64.1	2.40	0.19
5	69.6	2.73	0.36
5	69.8	2.35	0.23
5	69.9	2.43	0.27
5	69.9	2.25	0.30
5	75.1	2.75	0.52
10	85.4	2.35	0.14
10	86.7	2.40	0.1
10	95.5	2.45	0.23

TABLE III. Primary Creep Data $\varepsilon_1 \simeq 10^{C_i} t^{n_1}$ for Water-Saturated Westerly Granite as a Function of Stress-State.

$\sigma_2 = \sigma_3$ (10^3 psi)	σ_1 10^3 psi	Secondary Creep Rates, $sec.^{-1}$					
		$\dot{\varepsilon}_{1II}$	$-\dot{\varepsilon}_{II}$	$\dot{\varepsilon}_{3II}/\dot{\varepsilon}_{1II}$	$-\dot{\varepsilon}_{II}$	$\dot{\gamma}_{II}$	$-\dot{\varepsilon}_{II}/\dot{\gamma}_{II}$
0	19.3	10^{-13}	?	?	?	?	?
0	21.2	10^{-12}	?	?	?	?	?
0	23.2	10^{-11}	?	?	?	?	?
0	25.0	10^{-10}	?	?	?	?	?
0	30.0	10^{-8}	?	?	?	?	?
0	31.0	10^{-7}	?	?	?	?	?
0	33.0	10^{-6}	?	?	?	?	?
1	32.4	1.8×10^{-10}	6.21×10^{-10}	3.45	1.06×10^{-9}	8.01×10^{-10}	1.32
1	33.0	6.65×10^{-10}	?	?	?	?	?
1	36.3	1.26×10^{-9}	6.46×10^{-9}	5.13	1.17×10^{-9}	7.72×10^{-9}	1.51
1	40.2	2.82×10^{-8}	9.0×10^{-8}	3.19	1.52×10^{-7}	1.18×10^{-7}	1.29
5	58.8	3.97×10^{-10}	3.86×10^{-10}	0.97	3.75×10^{-10}	7.86×10^{-10}	0.48
5	62.7	1.56×10^{-10}	2.9×10^{-10}	1.86	4.24×10^{-10}	4.46×10^{-10}	0.95
5	64.1	5.64×10^{-10}	3.42×10^{-9}	6.06	5.28×10^{-9}	3.98×10^{-9}	1.58
5	69.6	1.03×10^{-8}	1.76×10^{-8}	1.71	2.49×10^{-8}	2.79×10^{-8}	0.89
5	69.8	1.98×10^{-9}	3.78×10^{-9}	1.91	5.58×10^{-9}	5.76×10^{-9}	0.97
5	69.9	4.27×10^{-10}	1.14×10^{-9}	2.67	1.85×10^{-9}	1.57×10^{-9}	1.18
5	69.9	3.44×10^{-10}	5.2×10^{-10}	1.12	7.0×10^{-10}	8.64×10^{-10}	0.81
5	75.1	1.13×10^{-7}	3.33×10^{-7}	2.96	5.34×10^{-7}	4.46×10^{-7}	1.20
10	85.4	8.63×10^{-9}	1.04×10^{-8}	1.20	1.22×10^{-8}	1.90×10^{-8}	0.64
10	86.7	4.5×10^{-10}	3.53×10^{-10}	0.78	2.56×10^{-10}	8.03×10^{-10}	0.32
10	95.5	6.66×10^{-10}	7.5×10^{-10}	1.13	8.74×10^{-10}	1.42×10^{-9}	0.62

TABLE IV. Secondary Creep Data for Water-Saturated w.g. as a Function of Stress State.

phenomena were distorted by strain hardening which occurred during the slow initial loading process (as opposed to instantaneous load application). For this reason the examination of the creep data from confining pressure tests concentrated on the secondary creep stage. All measured secondary creep rates for granite are listed in Table IV.

Some of the results in Table IV were cross-plotted in Figures 11 to 14 in an attempt to relate the secondary creep rates $\dot{\varepsilon}_{1II}$ to shear stress, confining pressure and mean stress. In Figure 11 the assumption was made that the secondary creep rate is of the order of 10^{-5}/sec. when the ultimate strength is reached in quasi-static compression. Best fits to the axial creep data in Figure 12 were used to construct curves of constant creep rate in the spaces $(\frac{\sigma_1 - \sigma_3}{2}, \sigma_3)$, $(\frac{\sigma_1 - \sigma_3}{2}, \sigma_m)$, and $(\frac{\sigma_1 - (\sigma_3 + C)}{2}, \sigma_m)$ in Figures 12 through 14. Figure 14 characterizes one of several unsuccessful attempts to "normalize" the experimental results.

A comparison of the data in Table IV suggests that the rates of lateral, volumetric and shear strains, $\dot{\varepsilon}_{3II}$, $\dot{\varepsilon}_{II}$ and $\dot{\gamma}_{II}$ exhibit the same trends with changes in the above variables as the secondary creep rate $\dot{\varepsilon}_{1II}$. This is indicated in Figure 15 where the shear stress is plotted versus the secondary volumetric and secondary shear creep rates.

For comparison of the creep behavior of rocks of different porosity, three creep experiments were conducted on water-saturated Nugget sandstone (7 per cent porosity) under 5,000 psi confining pressure, and at $\sigma_1 - \sigma_3$ = 49,700 psi and $\sigma_1 - \sigma_3$ = 56,200 psi, i.e. 0.81 and 0.92 times the ultimate strength in quasi-static compression. Creep curves ε_1 and ε_3 versus time for two specimens subjected to the same stress difference $\sigma_1 - \sigma_3$ = 49,700 psi are shown in Figures 16 and 17. Obviously, the results are drastically different.

σ_1 (10^3 psi)	$\varepsilon_{iI} \simeq 10^{C_{it}} n_i$ t in hrs				Secondary Creep Rates sec.$^{-1}$					
	C_1+6	n_i	C_2+6	n_2	$\dot{\varepsilon}_{1II}$	$-\dot{\varepsilon}_{3II}$	$-\dot{\varepsilon}_{3II}/\dot{\varepsilon}_{1II}$	γi_{II}	$-\dot{\varepsilon}_{II}$	$-\dot{\varepsilon}_{II}/\gamma_{II}$
22.4	1.83	0.06	1.88	0.30	7.5×10^{-12}	1.5×10^{-11}	1.97	2.25×10^{-11}	2.23×10^{-11}	0.99
26.05	1.60	0.14	2.68	0.35	4.48×10^{-11}	1.24×10^{-10}	2.77	1.69×10^{-10}	2.03×10^{-10}	1.20
28.0	1.65	0.15	2.0	0.15	2.51×10^{-11}	2.52×10^{-10}	10.03	2.77×10^{-10}	4.79×10^{-10}	1.73
28.0	1.0	0.21	1.03	0.44	2.66×10^{-10}	1.71×10^{-9}	6.42	1.98×10^{-9}	3.15×10^{-9}	1.59
28.3	2.62	0.14	1.73	0.30	6.37×10^{-10}	1.91×10^{-9}	3.00	2.55×10^{-9}	3.18×10^{-9}	1.25
29.0	1.80	0.25	2.15	0.46	4.78×10^{-11}	3.75×10^{-10}	7.85	4.23×10^{-10}	7.02×10^{-10}	1.66
29.9	1.72	0.34	2.30	0.50	1.88×10^{-8}	1.47×10^{-7}	7.82	1.66×10^{-7}	2.75×10^{-7}	1.66
30.0	1.65	0.48	3.45	0.75	1×10^{-7}	8.25×10^{-7}	8.25	9.25×10^{-7}	1.55×10^{-6}	1.68
30.2	2.68	0.40	3.45	0.50	1.48×10^{-7}	9.83×10^{-7}	6.64	1.13×10^{-6}	1.82×10^{-6}	1.61
31.0	?	?	2.2	0.66	?	4.08×10^{-8}	?	?	?	?
31.05	0.80	0.45	1.20	0.67	2.29×10^{-9}	1.6×10^{-8}	7.27	1.82×10^{-8}	2.98×10^{-8}	1.64
31.4	1.75	0.60	3.58	0.75	5.4×10^{-7}	2.44×10^{-6}	4.52	2.98×10^{-6}	4.35×10^{-6}	1.46
32.0	1.57	0.30	2.15	0.14	1.55×10^{-9}	7.41×10^{-9}	4.78	8.96×10^{-9}	1.33×10^{-8}	1.48
34.0	2.75	0.79	3.15	0.66	1.89×10^{-7}	4.88×10^{-7}	2.58	6.77×10^{-7}	7.87×10^{-7}	1.16

TABLE V. Creep Data for Air-Dry Westerly Granite in Uniaxial Compression.

σ_1 (10^3 psi)	$\varepsilon_{1II}{}^2\ 10^{C_i}\ t^{n_i}$				Secondary Creep Rates, sec.$^{-1}$/ Table V.					
	C_1+6	n_2	C_2+6	n_2	$\dot{\varepsilon}_{1II}$	$\dot{\varepsilon}_{3II}$	$-\dot{\varepsilon}_{3II}/\dot{\varepsilon}_{1II}$	$-\dot{\varepsilon}_{II}$	$\dot{\gamma}_{II}$	$-\dot{\varepsilon}_{II}/\dot{\gamma}_{II}$
22.5	1.64	0.28	1.88	0.29	7.2×10^{-12}	3.77×10^{-11}	5.24	6.8×10^{-11}	4.49×10^{-11}	1.51
25.2	2.15	0.14	2.33	0.19	2.0×10^{-11}	8.8×10^{-11}	4.4	1.56×10^{-10}	1.08×10^{-10}	1.44
26.2	2.30	0.13	2.51	0.32	7.3×10^{-11}	2.2×10^{-10}	3.0	3.67×10^{-10}	2.93×10^{-10}	1.25
28.0	1.52	0.13	1.94	0.34	2.3×10^{-10}	9.8×10^{-10}	4.36	1.73×10^{-9}	1.21×10^{-9}	1.43
28.0	2.28	0.11	2.40	0.30	8.8×10^{-11}	6.0×10^{-10}	6.82	1.11×10^{-9}	6.88×10^{-10}	1.61
28.3	2.88	0.52	3.28	0.47	2.4×10^{-7}	6.2×10^{-7}	2.58	1.0×10^{-6}	8.6×10^{-7}	1.16

TABLE VI. Creep Data for Air-Dry Nugget Sandstone in Uniaxial Compression.

Stress $-\sigma_1$ (10^3 psi)	Secondary Axial Creep Rate, $\dot{\varepsilon}_{1II}$ (sec^{-1})	Time to Failure (hrs)
1	8.55×10^{-12}	>1,200
1.1	not recorded	> 480
1.2	1.5×10^{-4}	40
1.2	2.1×10^{-11}	> 300
1.2	3.3×10^{-10}	4.5
1.2	3.2×10^{-9}	30
1.2	not recorded	72
1.3	data not resolvable	> 340
1.3	data not resolvable	> 610
1.4	3.1×10^{-8}	0.17
1.4	not recorded	0.33

TABLE VII. Secondary Creep Data, $\dot{\varepsilon}_{1II}$, and Failure Times for Air-Dry Westerly Granite in Uniaxial Tension.

This fact is attributed to time-dependent compaction and differences in loading histories; prior to deviatoric loading samples A and B were held under hydrostatic pressure for periods of 16 hours and 72 hours, respectively.

Creep Experiments in Uniaxial Compression

Creep experiments were performed in uniaxial compression on air-dry Westerly granite (14 tests) and Nugget sandstone (6 tests). The test durations ranged from 35 hours to 1,300 hours. Typical creep curves for both rocks were presented in an earlier report (1). All pertinent data obtained are presented in Tables V and VI. A comparison of the secondary creep rates $\dot{\varepsilon}_{III}$ of air-dry and water-saturated Westerly granite is shown in Figures 17 and 18. The results for water-saturated samples were generated in an earlier study (1). Primary creep results for air-dry and water-saturated granite are compared in Figure 19 assuming that $\dot{\varepsilon}_{iI} = 10^{C_i} t^{n_i}$.

Quasi-Static and Creep Experiments in Uniaxial Tension

Tension experiments were performed on air-dry Westerly granite only after Nugget sandstone was found to fail at widely fluctuating stress levels along weak bedding planes perpendicular to the specimen axes. Approximately one half of the granite tests had to be discarded because of fracture along the glue lines between the sample ends and the metal end-caps both during quasi-static loading and in creep. The mean quasi-static tensile strength of six granite specimens was 1,440 psi, plus 8.8 per cent minus 7.2 per cent of the sample mean. The wide range of "tensile strengths" is attributed to uneven loading. A typical quasi-static stress-strain curve is depicted in Figure 21.

Creep and creep fracture experiments were conducted in the range from 1,000 psi to 1,400 psi. The test durations varied between 0.3 and 1,200 hours. The few "valid" results obtained are summarized in Table VII and

suffice to demonstrate the tremondous data scatter. Lateral (circumferential) creep strains could never be resolved, i.e. they were less than 25×10^{-6}. The axial creep strain to failure varied from 3.8×10^{-4} at 1,400 psi stress and 5×10^{-4} at a stress of 1,200 psi.

Quasi-Static and Creep Experiments on Jointed Rock

Quasi-static and creep experiments were conducted on three specimens of air-dry or water-saturated Westerly granite each containing one unfilled joint inclined at 30^{0} relative to the direction of greatest compression. The quasi-static data provided estimates of the static coefficients of friction at the onset of macroscopic sliding which are indicated in Table VIII. They also permitted the average normal and shear displacements d_n and d_s on the joint to be determined as functions of the average normal and shear stresses on the joint σ_n and τ_n, respectively, (Figures 3, 22, and 23).

Creep tests on the joints were carried out under 3,000 psi confining pressure at (1) two levels of stress difference prior to the development of macroscopic slip, and (2) at a stress difference of 0.8 times the ultimate strength but after slip had occurred under quasi-static loading conditions and some gouge had accumulated. The results of test (1) are shown in Figure 24. No creep was observed in experiment (2) over a period of 24 hours.

Sample Number	Confining Pressure $\sigma_2 = \sigma_3$ (10^3 psi)	Coefficient Friction μ
J-2 (Air-Dry)	1	1.00
	3	0.90
	5	0.80
J-4 (Water saturated)	1	1.05
	3	0.86
J-3 (Water-saturated)	3	0.96

TABLE VIII. Coefficients of Friction for Joints (Artifically Induced Tension Fracture, Roughness, $\pm$0.020 in.) in Westerly Granite as a Function of Confining Pressure.

DISCUSSION

Creep Under Confining Pressure and in Uniaxial Compression

The presentation and discussion of the results of all creep tests is difficult for three reasons. (1) The number of data points in any category of experiments, confining pressure, uniaxial compression and uniaxial tension tests, is small and the results of repeated experiments is obscured by considerable scatter. If more data were to be generated it would be necessary that either the project duration be extended or that several tests stands be fabricated to multiply the data output per unit time. (2) The form of the relationship between the time-dependent strain components, ε_1, $\varepsilon_2=\varepsilon_3$, ε, or $\gamma = \varepsilon_1 - \varepsilon_3$ or between the time rates of the strain components on one hand and stress state (σ_1, $\sigma_2 = \sigma_3$, $\sigma_1 - \sigma_3$ σ_m) and time on the other is not readily recognized. (3) The presentation of some of the creep data is based on the assumption that the secondary creep rate is approximately 10^{-5}/sec. when the ultimate strength is reached in quasi-static compression. This assumption is reasonable but not unquestionable.

The inspection of all results which were gathered in confining pressure experiments leads to several key observations. Regardless of the magnitude of the creep strains in granite, obviously they are a non-linear function of stress. For example, Figures 11 and 12 demonstrate that a doubling of the stress difference increases the creep rate $\dot{\varepsilon}_{III}$ by factors of approximately five and an unknown multiple of five under constant confining pressure and fixed mean stress, respectively. It is equally apparent that the volumetric strain $\dot{\varepsilon}$ and the shear strain $\dot{\gamma}$ are of the same order of magnitude, i.e. neither can be neglected (Table III, Figure 15). The problem is further complicated by the observation that shear stress and volume strain are

functions both of the shear stress and the mean stress. It follows directly from Figure 15, for example, that a change of the shear stress at constant confining pressure or at constant mean stress will effect the volumetric strain quite markedly. In fact, Figure 15 suggests that the magnitude of the change in $\dot{\varepsilon}$ will exceed the amount of change in $\dot{\gamma}$ at shear stresses greater than the values at points A, B and C in Figure 15 at 1,000 psi, 5,000 psi and, 10,000 psi confining pressure. The coupling of shear strain and volumetric strains clearly provides further evidence that the time-dependent stress-strain behavior of granite is non-linear.

The creep response of Nugget sandstone finally indicates that creep in some rocks might be a result of competing effects. In Nugget sandstone these effects are likely related to simultaneous pore collapse and micro-cracking so as to produce net volume changes which are positive (dilatancy), negative (compaction) or zero depending on the previous stress history (Figures 16 and 17).

Essentially all creep in granite and Nugget sandstone was non-recoverable. The greatest amount of recovery at zero deviatoric stress over a 54 hour period amounted to 5 per cent of the total accumulated creep strain prior to unloading.

The comparative creep behavior of granite and sandstone in uniaxial compression and under confining pressure is suggested by the results for both air-dry and water-saturated specimens. Most notable the data in Table III and in Figures 11 through 14 indicate that the axial and lateral creep and with it the time-dependent changes of the volumetric and shear strains slow down as the confining pressure is raised. In addition, the ratios of lateral to axial strain and of volumetric to shear strains in creep drop markedly with increasing confining pressure. This is attested in Figure

15 by the progressive shift of the points A, B, and C at which $\dot{\varepsilon}_{II} = \dot{\gamma}_{II}$ to the right. Therefore, the observations of large ratios $\dot{\varepsilon}_{3II}/\dot{\varepsilon}_{1II}$, for example, in uniaxial compression are consistent with the trends seen in confining pressure experiments. If creep at stress levels above approximately half the ultimate strength is due to micro-cracking, then it is reasonable to assume that the change in the strain ratios $\dot{\varepsilon}_{3II}/\dot{\varepsilon}_{1II}$ etc. is primarily due to the change in micro-crack density, orientation of micro-cracks and possibly to a change in the mode of crack growth from cleavage to in-plane shear.

It is noted that volumetric and shear strains in uniaxial compression were measured on air-dry specimens only. Although the creep in these samples proceeded more slowly than in water-saturated specimens it is assumed that the ratios of these strains are comparable no matter how much water is present. Hence, the above comparison of results for water-saturated rock under confining pressure and for air-dry samples in uniaxial compression is considered permissible.

The effect of water is demonstrated by the results in Figures 18 through 20. In Figures 18 and 19 the logarithm of the secondary creep rate $\dot{\varepsilon}_{1II}$ is plotted versus the uniaxial compressive stress σ_1 (Figure 18) and versus the lagarithm of the stress (Figure 19). The data have too much scatter in both graphs to determine whether the relationship between creep strain and stress, is an exponential or a power function of stress. Nevertheless, it appears that the difference in water content between air-dry and water-saturated specimens amounts to approximately two orders of magnitude in the secondary creep rates at any given stress level (Figure 18). Because the per cent difference in the ultimate strength of air-dry and water-saturated granite is nearly the same regardless of the magnitude of the confining pressure, it is likely that the effects which are indicated by the data in Figures 18, 19 and 20 are not

restricted to uniaxial compression.

Creep in Uniaxial Tension

Relatively little can yet be said about the creep of granite in uniaxial tension. Creep may again be divided into primary, secondary and tertiary stages if tertiary creep is interpreted as the onset of fracture. Without exception the transition between secondary creep and fracture lasted no more than a few minutes. Lateral strains $\varepsilon_3 = \varepsilon_2$ were always too small to be resolved. Axial creep proceeded at varying rates between 10^{-12}/sec. and 10^{-9}/sec. The greatest accumulated strain was 5×10^{-4} prior to fracture.

Response of Joints

The data on jointed granite clearly demonstrates the usefulness of standard confining pressure experiments to determine the mechanical properties of joints unde. quasi-static as well as constant loading conditions. Data on the relationship between normal and shear stress acting on joints and associated average normal and shear displacements had previously been obtained only in direct shear tests.

The few results which were attained in this study agree with the well known fact that open joints are both considerably weaker and more compliant than competent rock. However, surprisingly the joint compliances (one divided by joint stiffness) which were measured under confining pressure were less than the joint compliances commonly recorded in direct shear experiments. This discrepancy will have to be resolved considering that the two types of experiments employ different loading paths and that the superimposed hydrostatic pressure in confining pressure experiments tends to provide stronger interlocking of asparities along the joint surfaces.

According to the results of Table VIII it appears that the presence of water increases the strength of joints in granite. This observation may be

merely related to experimental scatter. However, it seems to be in line with results published by Swolfs.

Below the ultimate strength the influence of time on the deformation of unfilled rough joints was limited to negligible slip of less than 10^{-3} over a period of eight hours. No further joint motion was observed between eight and thirty-two hours when the creep experiments were terminated. Zero joint deformation was measured on a joint which had previously been loaded to the ultimate strength under 3,000 psi confining pressure.

At the end of each creep experiment the axial sample load was raised to the ultimate strength under constant confining pressure, and the coefficient of sliding friction was calculated. This friction data suggests that the coefficient of sliding friction increased slightly on rough essentially clean surfaces as a function of time during which the joint stresses are held fixed. The friction coefficient appeared to remain unaltered when the joint surfaces contained some powdery detritus as a result of quasi-statically induced slip in earlier phases of the experiments.

Time-Dependent Fracture

Creep fracture, times-to-failure and strains-to-failure were observed in only four experiments under 1,000 psi and 5,000 psi confining pressure at stress differences which ranged from 75 per cent to 96 per cent of the ultimate strength. The failure times varied between eight hours and 120 hours. In all experiments creep proceeded stably even after the total accumulated strains had reached magnitudes which were up to five times greater than the failure strains in uniaxial compression at equivalent levels of stress difference, for example 0.8 times the ultimate strength. Because of the small number of creep fracture observations and because of the lack of complete sets of complete stress-strain curves it is impossible to extrapolate the few creep fracture results or to prove the validity of a hypothesis which provided

upper bound estimates for the fracture times of three rock types in uniaxial compression. This hypothesis is based on the assumption that time-dependent failure occurs when rock has been strained a critical amount. Moreover, it stipulates that the greatest allowable strain prior to fracture under constant environmental conditions is primarily a function of the state of stress. This means that the time-dependent failure of rock might be predicted by comparing the time-dependent deformations with the allowable strains. The time-dependent strains can be calculated from suitable constitutive equations. Upper bounds of the allowable strains in turn are established in controlled quasi-static experiments as the difference between the pre-failure strains along the ascending branch of complete stress-strain curves and the post-failure strains along the descending branch of complete stress-strain curves.

Although the validity of the above hypothesis could not be adequately tested under confining pressure or in uniaxial tension, there are at least two reasons which still suggest that it has merit. (1) In three tests on granite under 1,000 psi confining pressure the strains to failure, ε_1 and $\varepsilon_2 = \varepsilon_2$ agreed very closely with the "allowable strains, e.g. $\varepsilon_1 = \varepsilon_q'$ (Figure 5). ε_q' in Figure 5 equals the axial strain difference between the pre- and post-failure strains at the same stress difference in quasi-static compression for water-saturated Westerly granite under 1,000 psi confining pressure. (2) Published complete stress-strain curves for air-dry Westerly granite (18) suggest that the upper bound of the allowable strain ε_q' increases as the confining pressure is raised. For example, when the stress difference $\sigma_1 - \sigma_3$ is 75 per cent of the ultimate strength, ε_q' increases from approximately 6×10^{-4} in uniaxial compression to 4×10^{-3} under 3,000 psi confining pressure and to approximately 6×10^{-3} under 12,000 psi confining pressure. Considering that the allowable strain ε_q' becomes greater and that the creep "slows down"

with increasing confining pressure, it appears reasonable to postulate that creep fracture is a much less likely under confining pressure than it is in uniaxial compression. This reasoning might well explain why creep fracture generally did not occur in our confining pressure experiments.

Obviously, the prediction of creep fracture in tension is open to question by any prediction scheme. The tests on granite merely suggest that the existence of a stress level, here 1,200 psi or 83 per cent of the uniaxial tensile strength, below which creep fracture is unlikely to develop in air-dry specimens. This apparent cut-off stress is probably sensitive to water content.

IDENTIFICATION OF FABRIC DAMAGE

The quantitative characterization of fabric damage due to localized rock fracture is an exceedingly difficult task. Once a specimen has reached the ultimate strength or has undergone a substantial amount of creep it is usually easy to recognize "some signs" of damage. For example, both specimens in Figure 25 exhibit sets of incipient shear fractures which are visible on the sample surfaces. However, to date all efforts to express such evidence of localized failure in terms of numbers which are readily derived in ultrasonic velocity tests, resistivity experiments or others have met with limited success at best. Most importantly, no way has yet been found to relate rock damage uniquely to a given stress state or loading history provided that such one-to-one relationships exist.

In this study fracture damage identifications were sought in two ways. (1) Polished sample sections were prepared from five granite and two sandstone specimens. These polished sections were viewed under a microscope both before and after the sections had been treated with a fluorescent die. (2) Ultrasonic velocity measurements (V_p) were carried out on seven specimens. On each specimen velocities were determined along four directions spaced at 45^o intervals perpendicular to the direction of greatest compression. Measurements were made on undeformed specimens (standards) and on samples which had been deformed quasi-statically and in creep.

All microscopic observations which included measurements of crack densities and micro-crack orientations proved to be totally inconclusive. Above all, it was impossible to draw unambiguous distinctions between cracks and open or closed grain boundaries which gave even surfaces of undeformed specimens a "crushed" appearance. It is suspected that this confusion is at least partly due to poor polishing which was handled commercially and,

therefore, could not be adequately controlled.

The value of all ultrasonic measurement is equally in question. They merely confirmed what could be observed directly. At 5,000 psi confining pressure, granite specimen No. 71 (Figure 25(a)) which had been deformed just beyond the ultimate strength, was more intensely fractured than specimen No. 107 which had been loaded to only 98 per cent of the ultimate strength. Hence the ultrasonic velocities in sample No. 71 perpendicular to the direction of greatest compression were lower than the velocities along equivalent paths in sample No. 107 (Figure 26). The velocities in specimen No. 103 (Figure 25(b)) which had undergone creep for 375 hours at a stress difference of 0.8 times the ultimate strength, lay between those in samples 107 and 71 (Figure 26). This observation could have been predicted from a cursory visual inspection of the specimen after the completion of the experiments. It strengthens earlier contentions that creep at high stress is dominated by micro-cracking. However, it says nothing about the details of the fracture patterns, about the similarity between micro-cracking in creep and quasi-static loading experiments or about methods which might be suitable to predict impending time-dependent rock fracture in situ.

SUMMARY AND CONCLUSIONS

This research had the very practical objective to evaluate whether or not time-dependent deformation and failure of rocks need to be considered in the total design of underground structures. To achieve this objective quasi-static, creep and creep-to-fracture experiments were conducted on air-dried and water saturated Westerly granite, Nugget sandstone and Tennessee marble under three different stress states: Uniaxial compression, compression with superimposed confining pressure and uniaxial tension. Both axial and lateral strain measurements were made in all experiments.

The results of these tests indicate that time-dependent effects of the rock types studied were noticeable, particularly in the water saturated state. However, these effects were subordinate when compared with the instantaneous rock response. Time-dependent deformation and the likelihood for time-dependent failure decreases drastically with confining pressure. Thus, in field situations time-dependent phenomena are considered appreciable only in the immediate vicinity of underground structures where at least one of the principal stresses is near zero. Time-dependent deformation and failure could become potentially hazardous at elevated pore pressure, i.e. if the effective mean stress is small.

Due to constraints in time and funding and because the influence of time in granite, sandstone and marble was judged subordinate, no efforts were made to model the observed time-dependent response. However, all data suggest that the observed volume and shear strains are complicated non-linear functions of shear stress, mean stress and time which do not obey any of numerous published mathematical models proposed for rocks to data. Specifically, the results suggest that valid time-dependent stress-strain relations will have to be based on complete strain measurements under

several different stress states. Uniaxial loading experiments and measurements of one strain component by themselves are inadequate and misleading.

It is emphasized that the above conclusions pertain to three specific rock types. While the behavior of these three rock types might be qualitatively representative for a large class of so-called hard rocks, the results presented here do not always apply, for example to shales or to rock salt. Furthermore, the data in this report are restricted to room temperature behavior and the validity of the effective stress law was implied but remains unproven.

REFERENCES

1. Wawersik, W. R., and W.S. Brown, "Creep Fracture of Rock in Uniaxial Compression." Final Report ARPA Contract No. H0110054; UTEC ME 71-242, University of Utah. 1971.

2. Rutter, E. H., "The Effects of Strain Rate Changes on the Strength and Ductility of Solenhofen Limestone at Low Temperatuee and Confining Pressure." International Journal of Rock Mechanics and Mineral Science, 9, 2, 1972.

3. Rutter, E. H., "On the Creep Testing of Rocks under Constant Stress and Constant Force." ibid.

4. Lindholm, E. S., "A Study of the Dynamic Strength and Fracture Properties of Rock." Semi-Annual Technical Report, ARPA Contract No. H0220063, Southwest Research INstitute, 1973.

5. Lai, James S., "Investigation of Bilinar Thermoviscoelastic Behavior of Rocks." Final Report, ARPA Contract No. H-220009, UTEC CE 73-128, University of Utah, 1973.

6. Heard, H. C., and Raleigh, C. B., "Steady State Flow in Marble at 500^{o} to 800^{o}C." Geologic Society American Bulletin, 83, 1973.

7. Rutter, E. H., The Effects of Temperature, Confining Pressure, Strain Rate and Interstitial Water in the Rheological Behavior of Calcite Rocks." Proceedings of the Fourteenth Symposium on Rock Mechanics, ASCE, 1973.

8. Swolfs, H. S., "Chemical Effects of Pore Fluids on Rock Properties."

9. McCarter, M. K., and Willson, J. E., "Strength Versus Energy Dissipation in Sandstone." Proceedings of the Fourteenth Symposium on Rock Mechanics, ASCE, 1972.

10. Scholz, C. H., "Static Fatigue of Quartz." Journal of Geophysical Research 77, 11, 1972.

11. Kennedy, B. A., and Niemeyer, K. E., "Slope Monitoring Systems Used in the Prediction of a Major Slope Failure at the Chuquicamata Mine, Chile." South African Institute of Mining, Meteorology, Johannesburg, 83, 1972.

12. Haimson, B., and Kim, C. M., and Tharp, T. M., "Tensile and Compressive Cyclic Stresses in Rock." Proceedings of the Fourteenth Symposium on Rock Mechanics, ASCE, 1972.

13. Haimson, B., and Kim, C. M., "Mechanical Behavior of Rock Under Cyclic Fatigue." Proceedings of the Thirteenth Symposium on Rock Mechanics, ASCE, 1972.

14. Peng, S., and Podnieks, E. R., "Relaxation and the Behavior of Failed Rocks." International Journal of Rock Mechanics and Mineral Science, 9, 6, 1972.

15. Handin, J., "Mechanical Properties of Rocks Affecting Earthquake Generation." Texas A&M Research Foundation, Texas A&M University, 1972.

16. Dietrich, J. H., "Time-Dependent Friction in Rocks." Journal of Geophysical Research, 77, 20, 1972.

17. Crouch, S. L., "Experimental Determination of Volumetric Strains in Failed Rocks." International Journal of Rock Mechanics and Mineral Science, 7, 5, 1970.

18. Wawersik, W. R., and Brace, W. S., "Post-Failure Behavior of Granite and Diabase." Rock Mechanics, 3, 3, 1971.

19. Appended References.

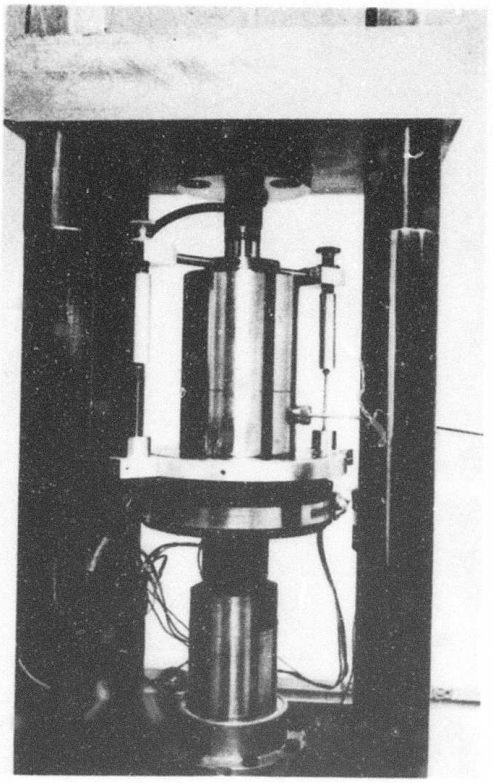

(a)

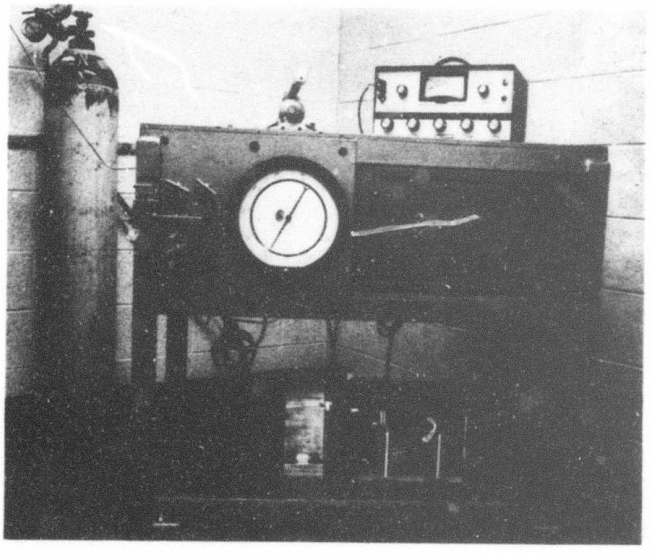

(b)

FIGURE 1. Experimental Equipment (a) Pressure Vessel; (b) Pressure Regulator and Servo-Control System; (c) Differential Pressure Gauge; (d) Tension Apparatus

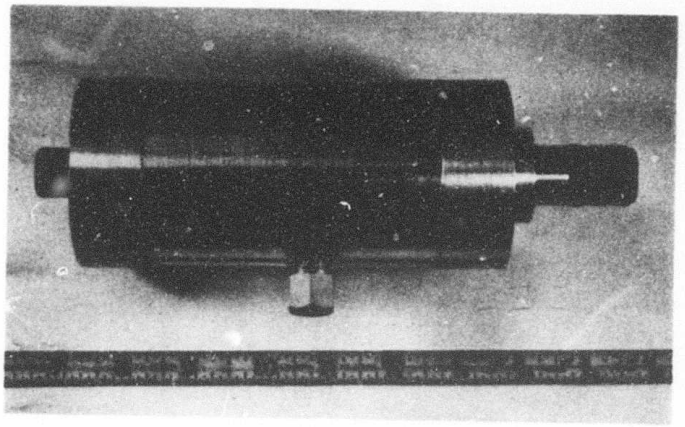

(c)

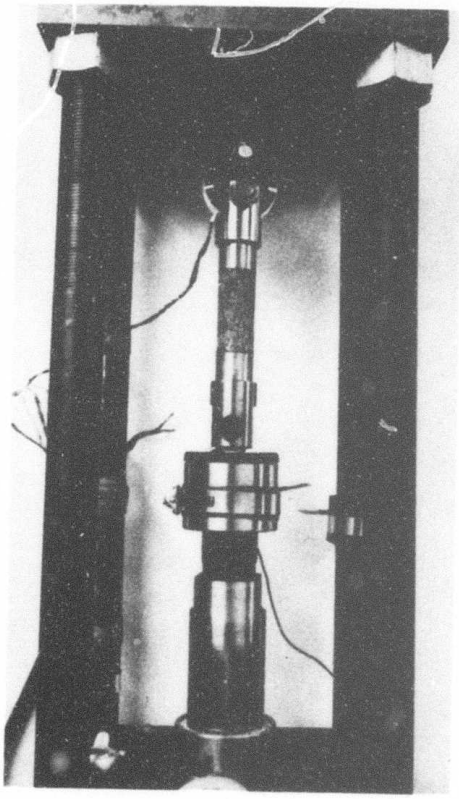

(d)

FIGURE 1. Experimental Equipment (a) Pressure Vessel; (b) Pressure Regulator and Servo-Control System; (c) Differential Pressure Gauge; (d) Tension Apparatus

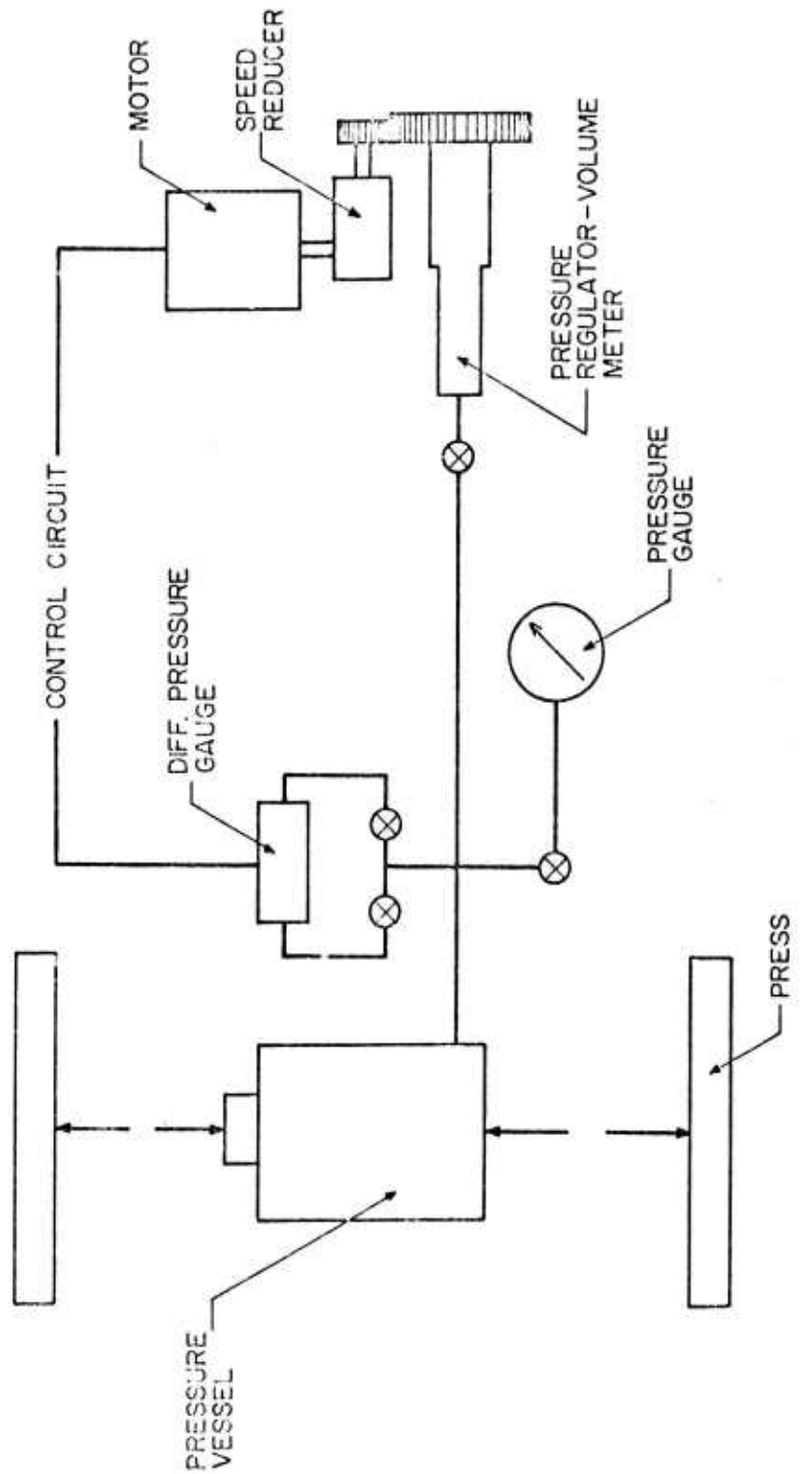

FIGURE 2. Schematic of Confining Pressure System.

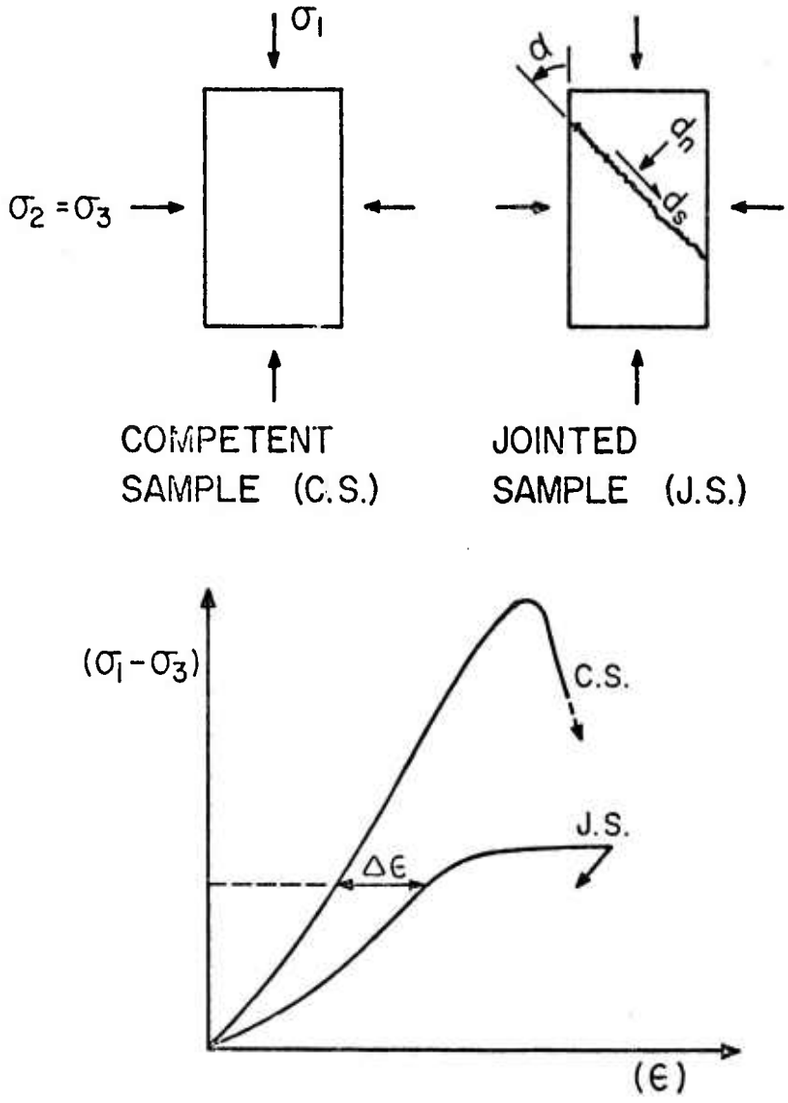

FIGURE 3. Schematic Comparison of Stress-Strain Responses of Competent and Jointed Rock.

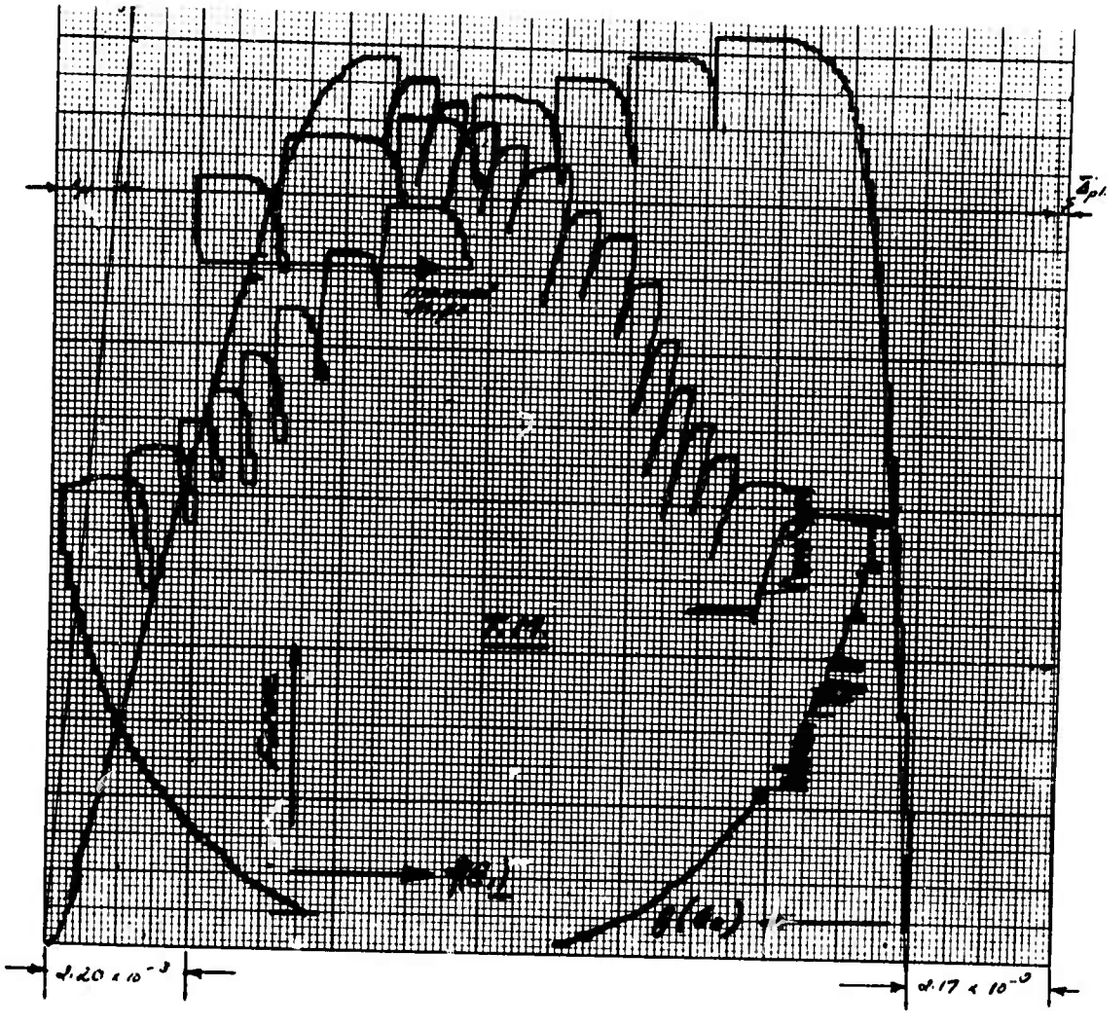

FIGURE 4. Original Record of Force Versus Axial and Radial Strain (Displacement) for Tennessee Marble Subjected to 1,000 psi Confining Pressure (Strain Rate $\dot{\varepsilon}_1 \approx 10^{-5}$/sec.)

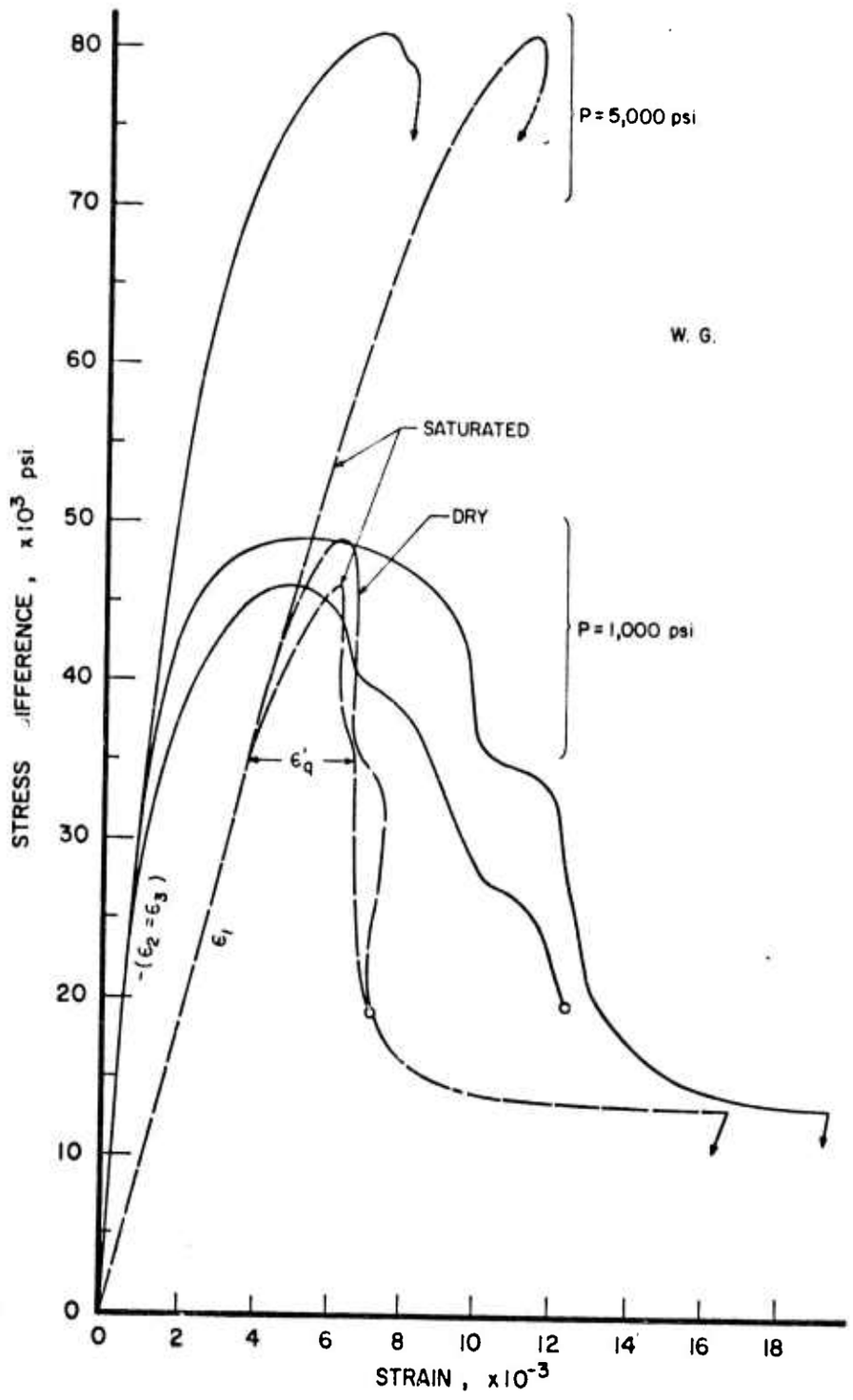

FIGURE 5. Quasi-Static Stress Strain Curves for Westerly Granite under Confining Pressure of 1,000 psi and 5,000 psi (strain rate $\dot{\epsilon}_1 \approx 10^{-5}$/sec.)

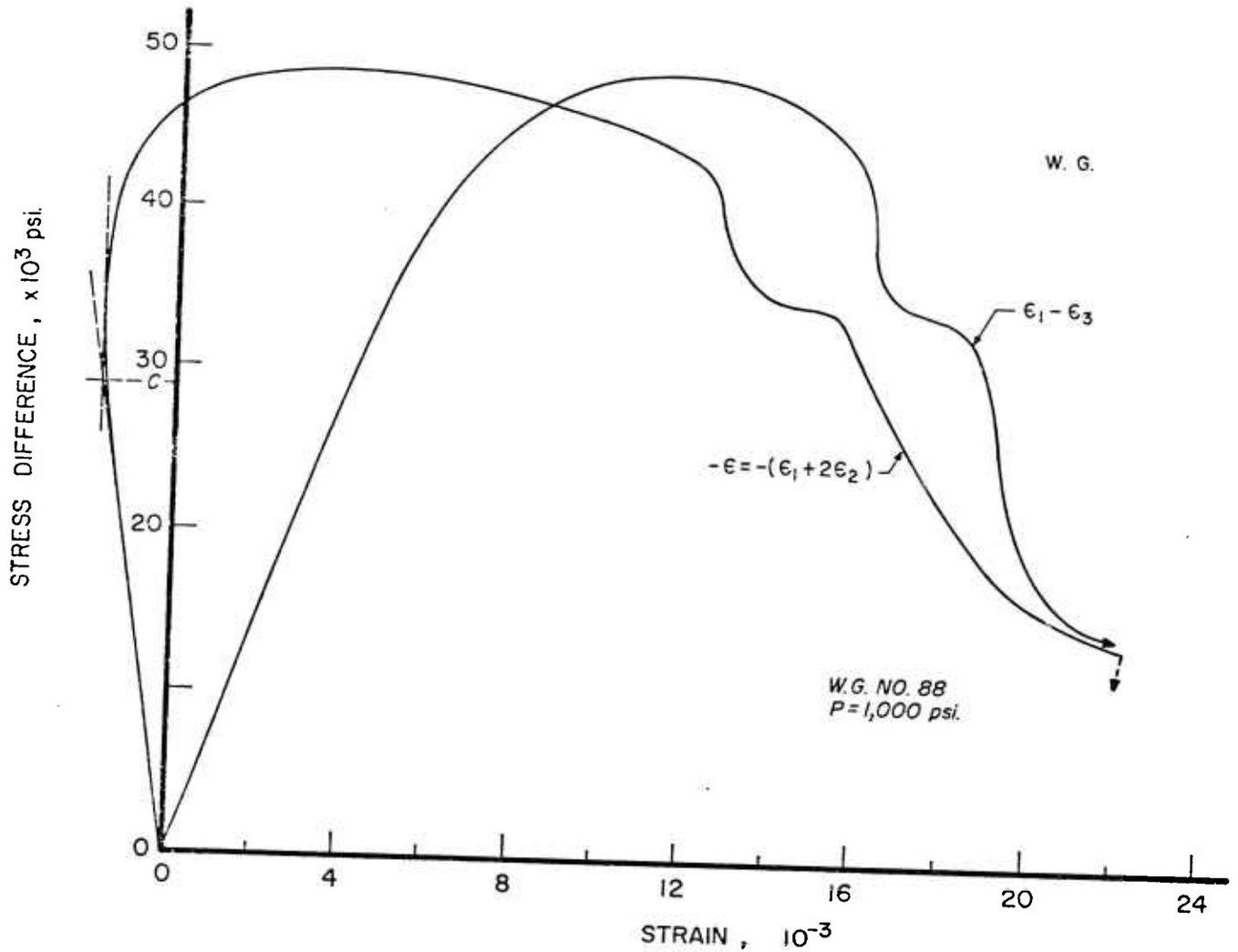

FIGURE 6. Stress Difference Versus Volumetric and Shear Strain for Air-Dry Westerly Granite in Quasi-Static Experiment at 1,000 psi Confining Pressure.

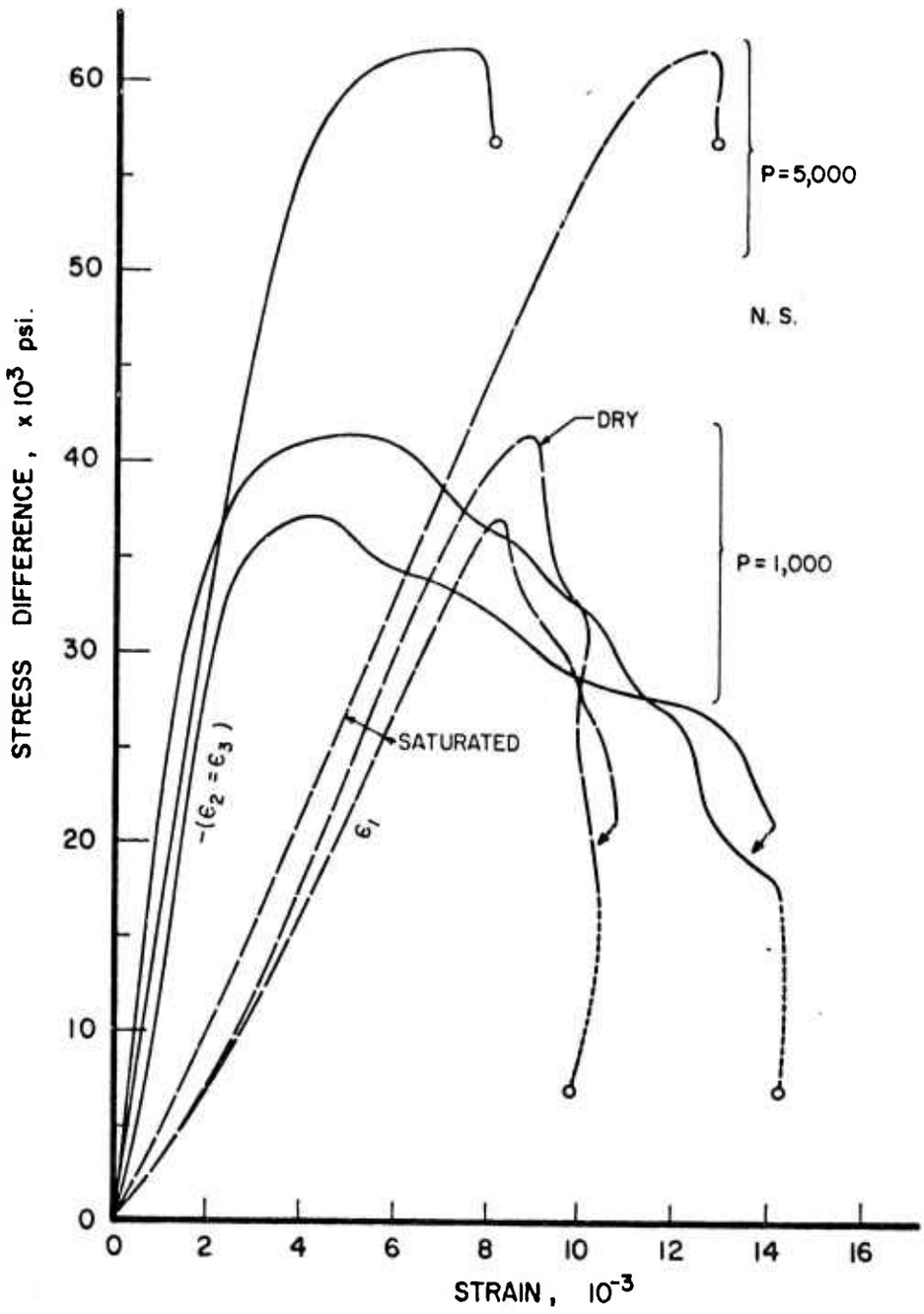

FIGURE 7. Quasi-Static Stress-Strain Curves for Nugget Sandstone under Confining Pressure of 1,000 pis and 5,000 psi (strain rate $\dot{\varepsilon}_1 \approx 10^{-5}$/sec.)

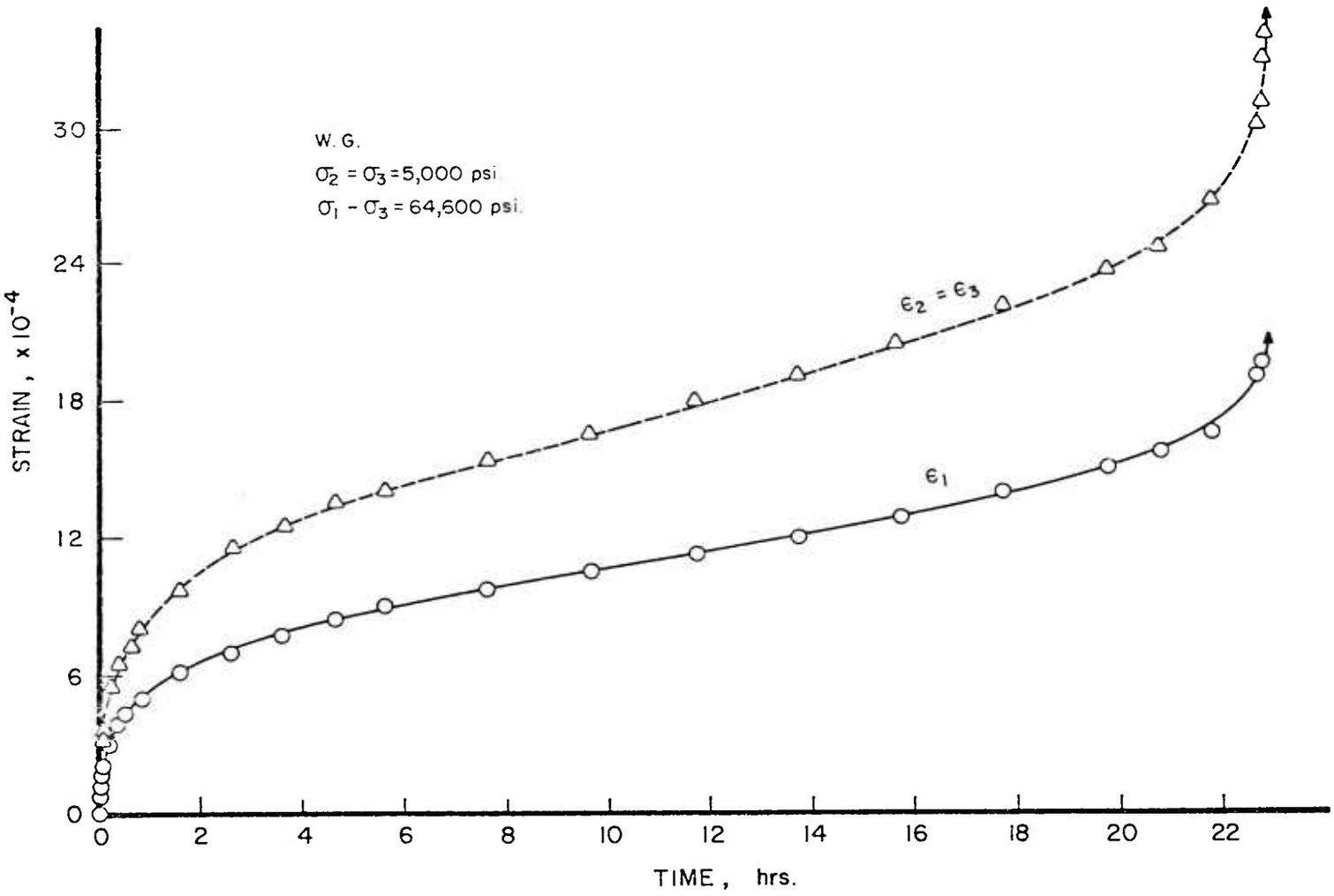

FIGURE 8. Creep Curves for Water-Saturated Westerly Granite subjected to Stress Difference $\sigma_1 - \sigma_3$ = 64,600 psi (446/MN/m^2) at 5,000 psi (34.5MN/m^2) confining pressure.

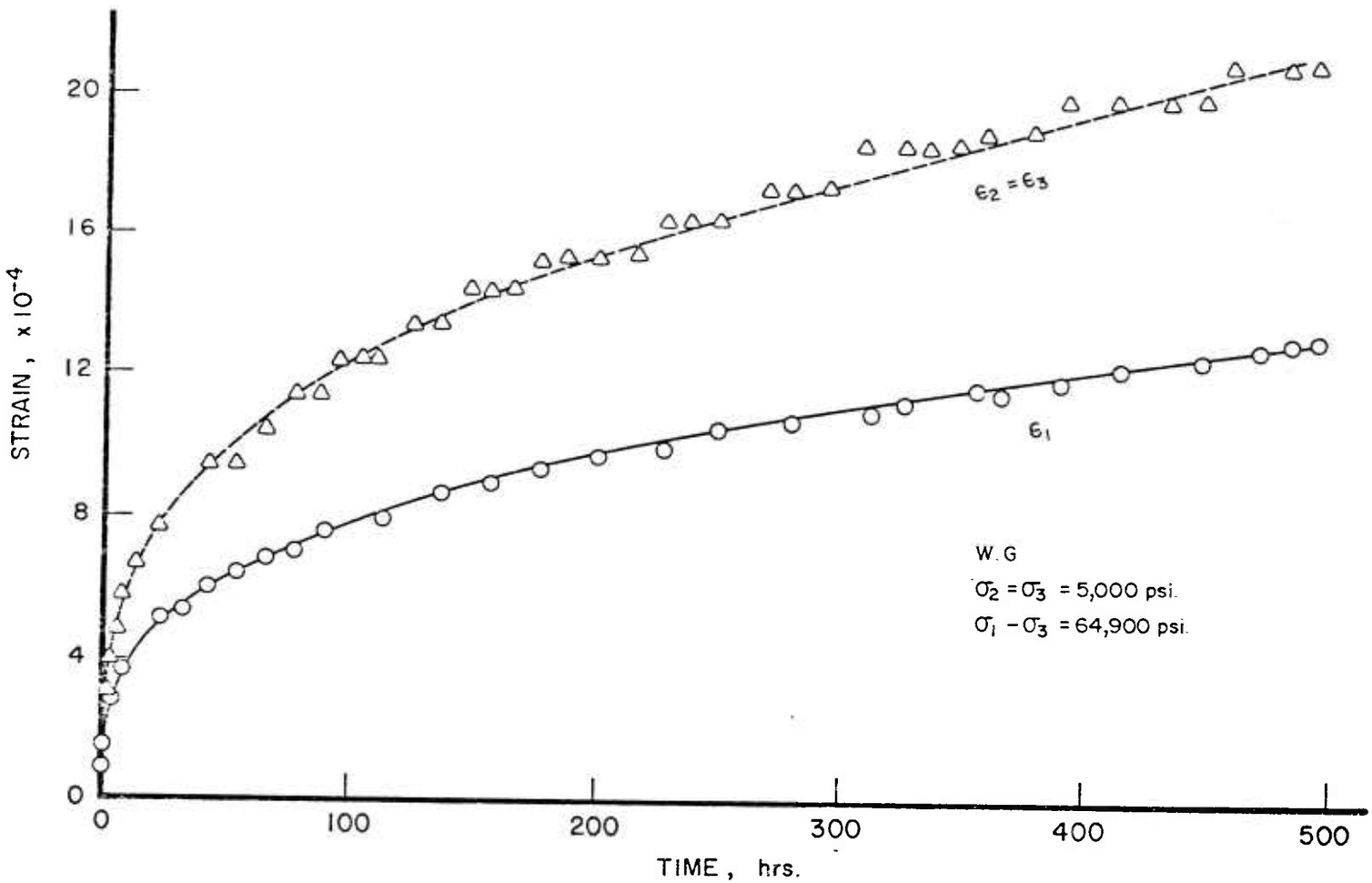

FIGURE 9. Creep Curves for Water-Saturated Westerly Granite Subjected to Stress Difference $\sigma_1 - \sigma_3$ = 64,900 psi at (446 MN/^{2}) at 5,000 psi (34.5 MN/m^2) confining pressure.

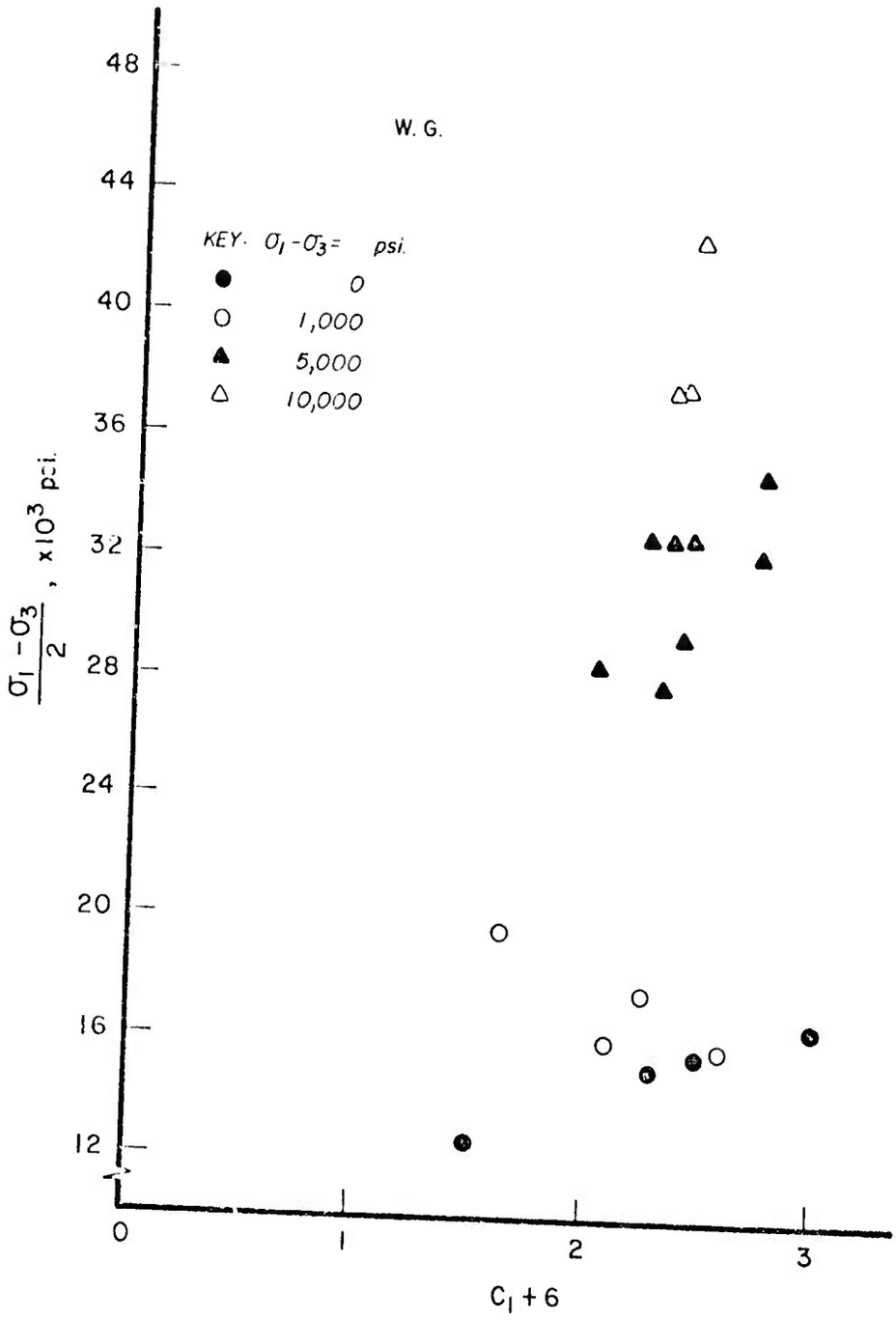

FIGURE 10. Some Primary Data for Water Saturated Westerly Granite as a Function of Shear Stress and Confining Pressure Assuming $\varepsilon_{iI} = 10 C_i t^{ni}$; n = .28.

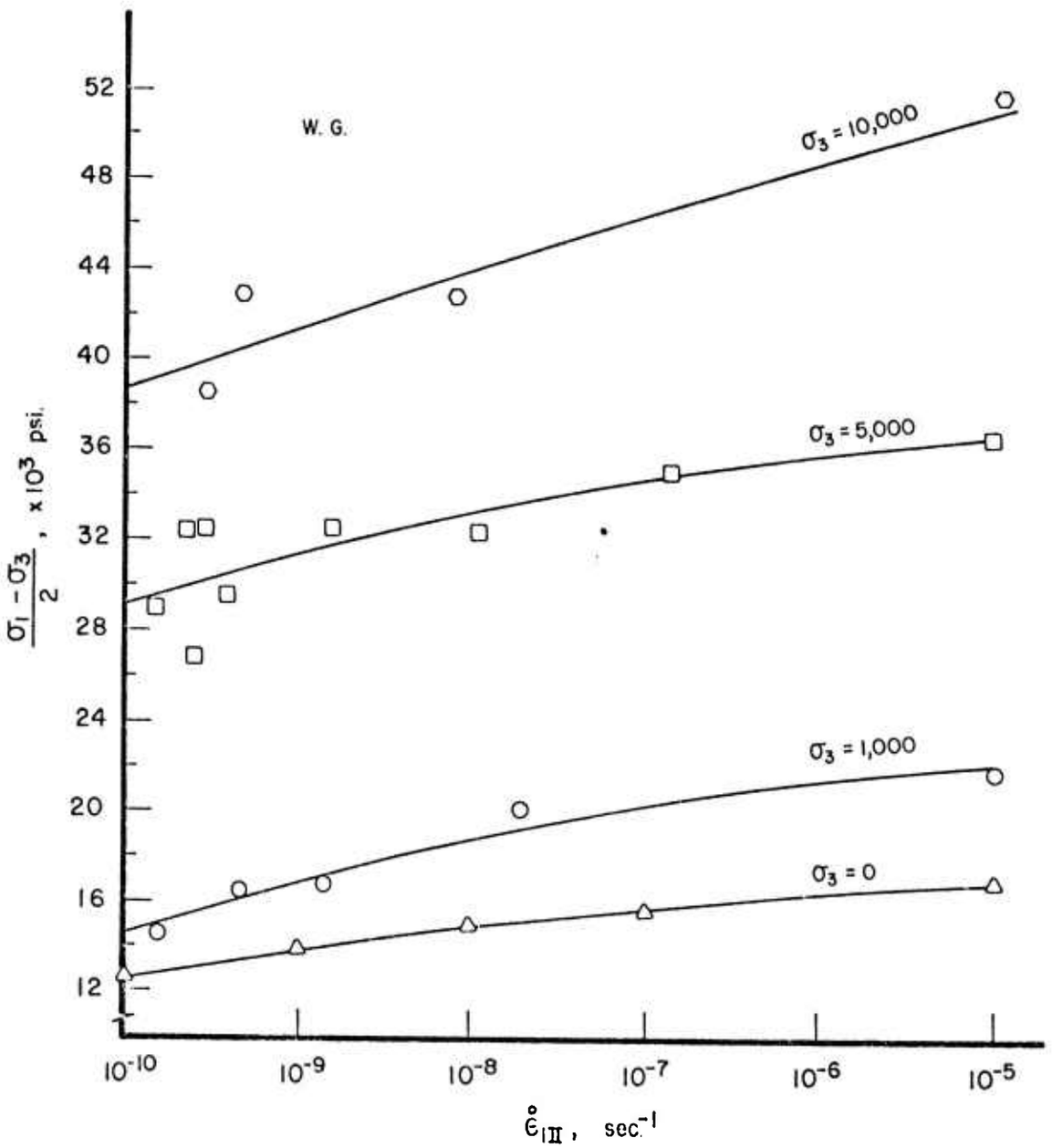

FIGURE 11. Shear Stress Versus Secondary Creep Rate $\dot{\epsilon}_{II}$ for Water-Saturated Westerly Granite at Confining Pressures up to 10,000 psi (69 MN/m^2).

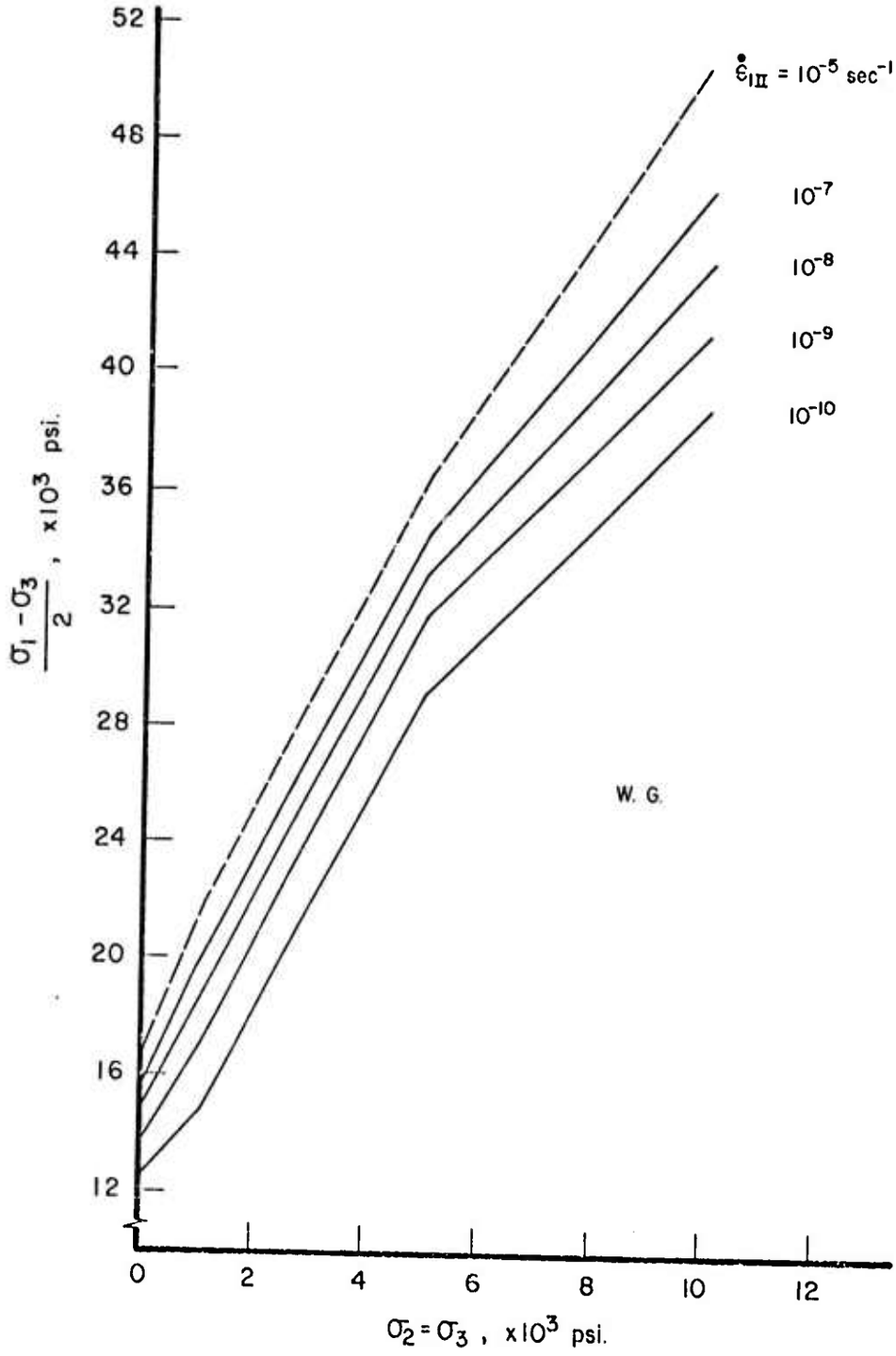

FIGURE 12. Curves of Constant Secondary Creep Rate $\dot{\varepsilon}_{III}$ for Water-Saturated Westerly Granite in the Space $(\frac{\sigma_1 - \sigma_3}{2}, \sigma_3)$.

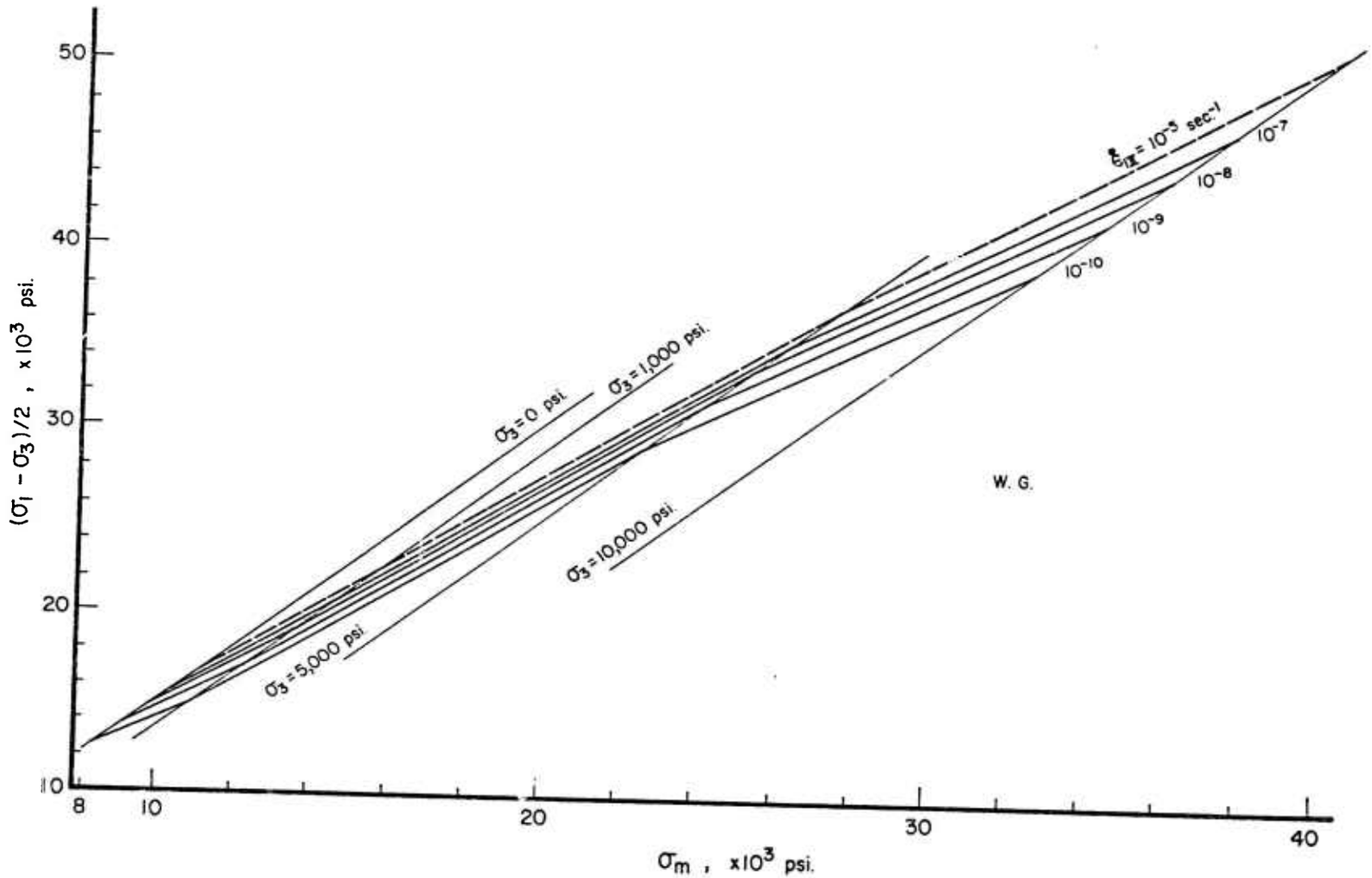

FIGURE 13. Curves of Constant Secondary Creep Rate $\dot{\varepsilon}_{III}$ for Water-Saturated Westerly Granite in the Space $\left(\frac{\sigma_1-\sigma_3}{2}, \sigma_m\right)$; $\sigma_m = 1/3(\sigma_1+\sigma_2+\sigma_3)$.

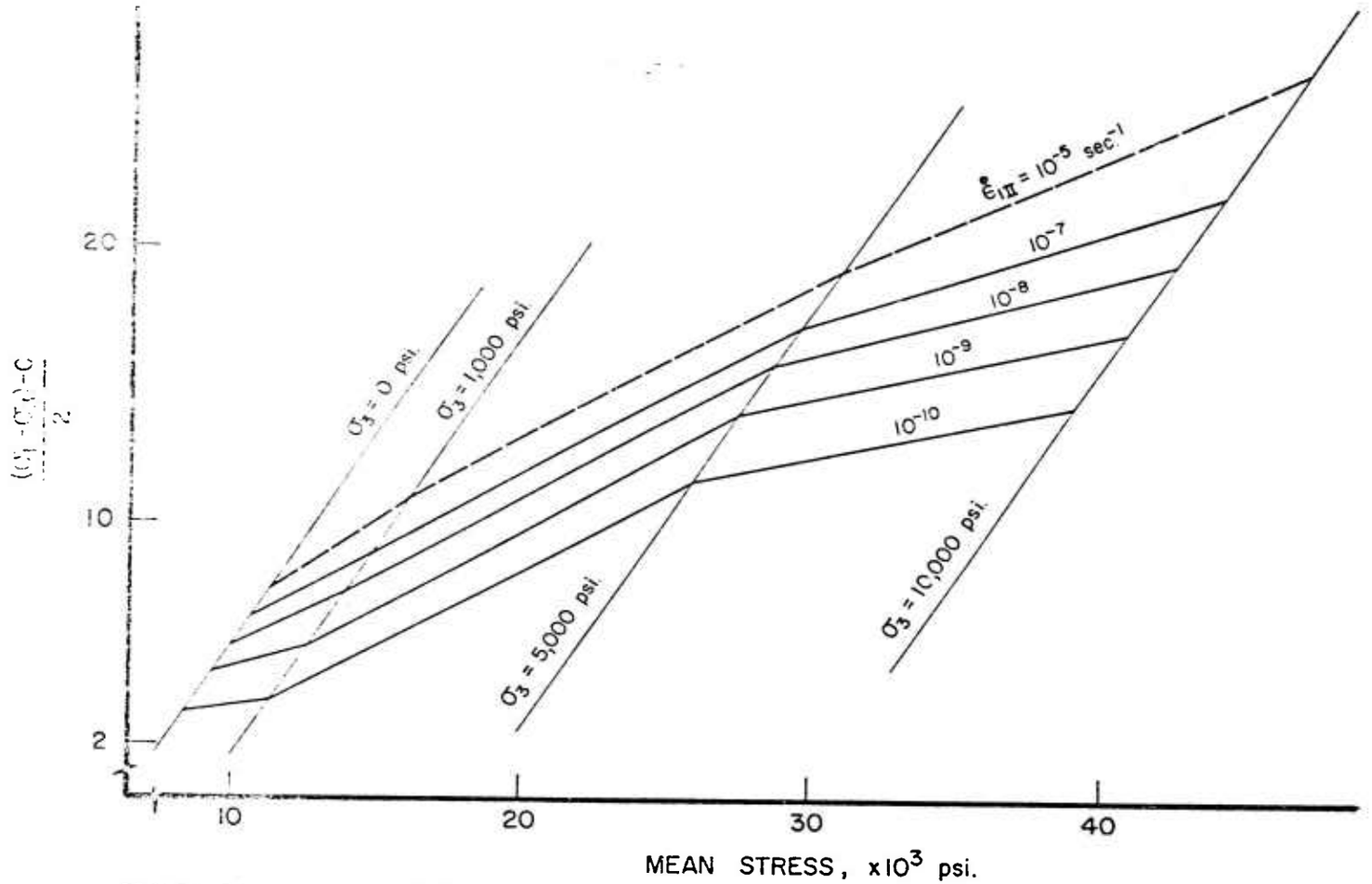

FIGURE 14. Curves of Constant Secondary Creep Rate $\dot{\varepsilon}_{III}$ for Water-Saturated Westerly Granite in the Space$((\sigma_1-(\sigma_3+C)/2, \sigma_m)$; $\sigma_m = 1/3\ (\sigma_1+\sigma_2+\sigma_3)$; C Denotes the Stress Difference at which Micro-Cracking is Assumed to Commence in Quasi-Static Compression at Strain Rate $\dot{\varepsilon}_1 \simeq 10^{-5}$/sec.

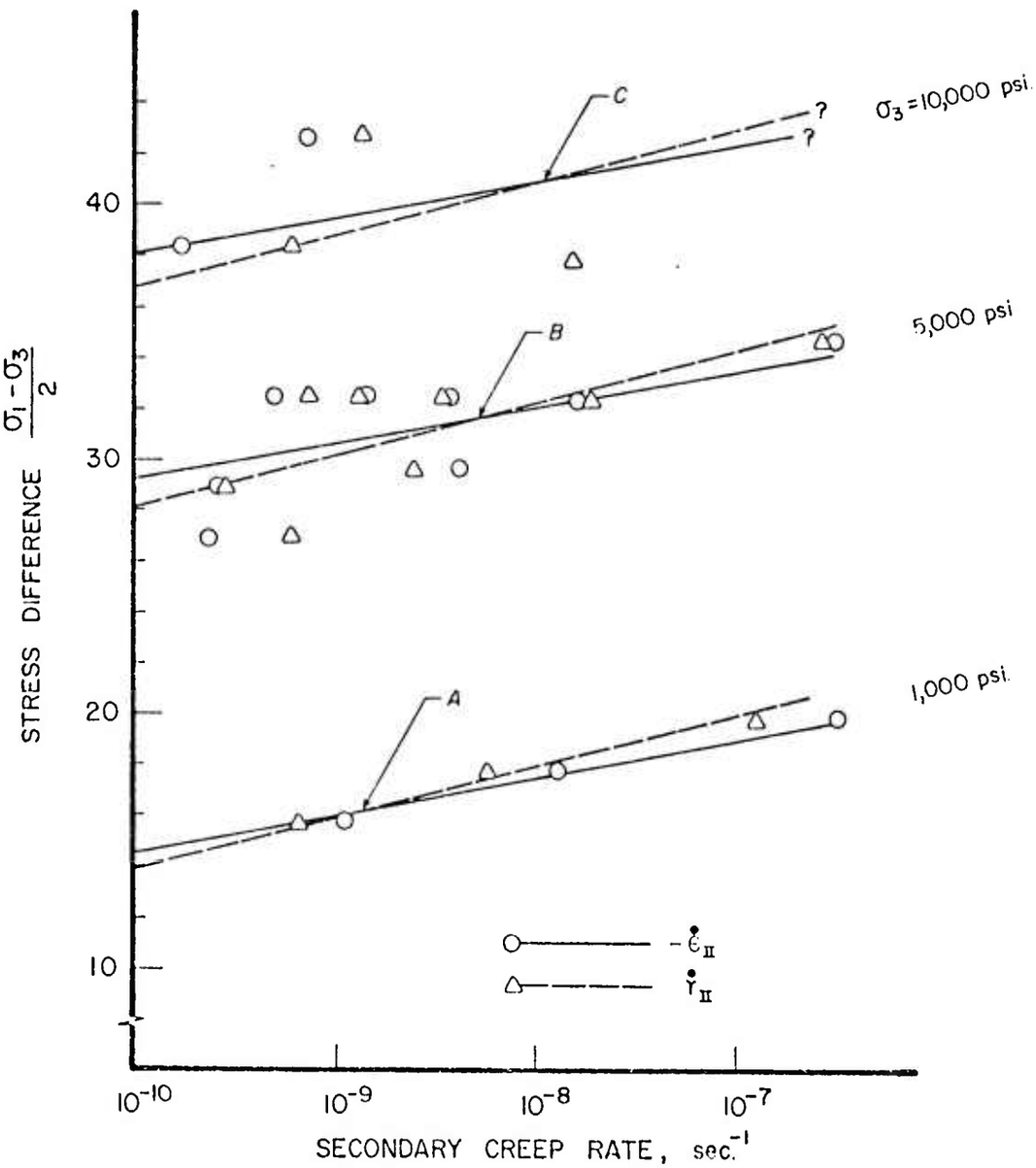

FIGURE 15. Shear Stress Versus the Time Rate of Change of Volumetric and Shear Strains during Secondary Creep for Water-Saturated Westerly Granite at 1,000 psi (6.9 MN/m^2) to 10,000 psi (69 MN/m^2) confining pressure.

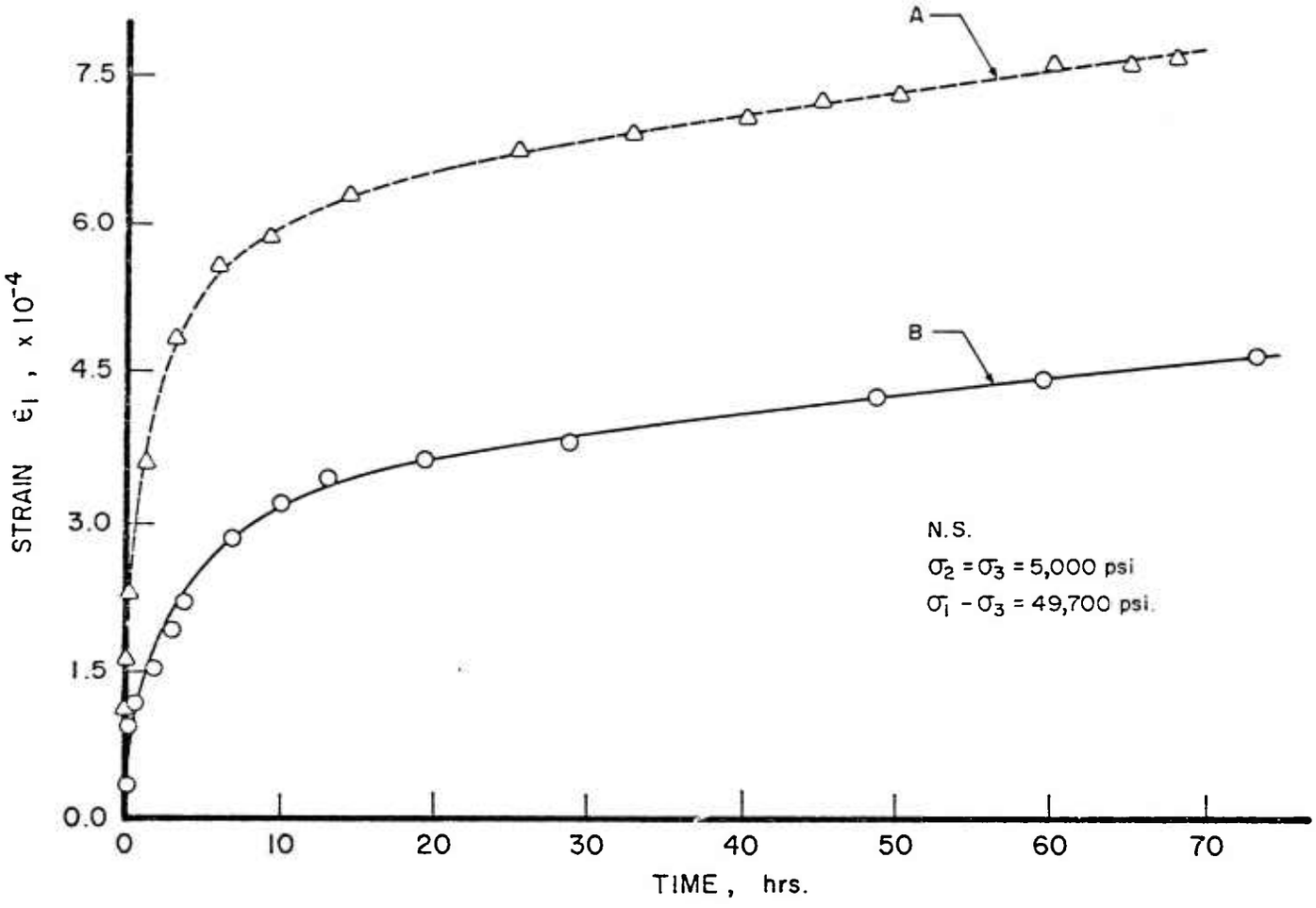

FIGURE 16. Creep Curves ϵ_1 versus Time for Water-Saturated Nugget Sandstone at $\sigma_1 - \sigma_3$ = 49,700 psi (343 MN/m^2 and 5,000 psi (34.5 MN/m^2) Confining Pressure. Stress Histories prior to Deviatoric Loading: Sample A - 5,000 psi (34.5 MN/m^2) Hydrostatic Pressure for 16 hours; Sample B - 5,000 psi (34.5 MN/m^2) Hydrostatic Pressure for 72 hours.

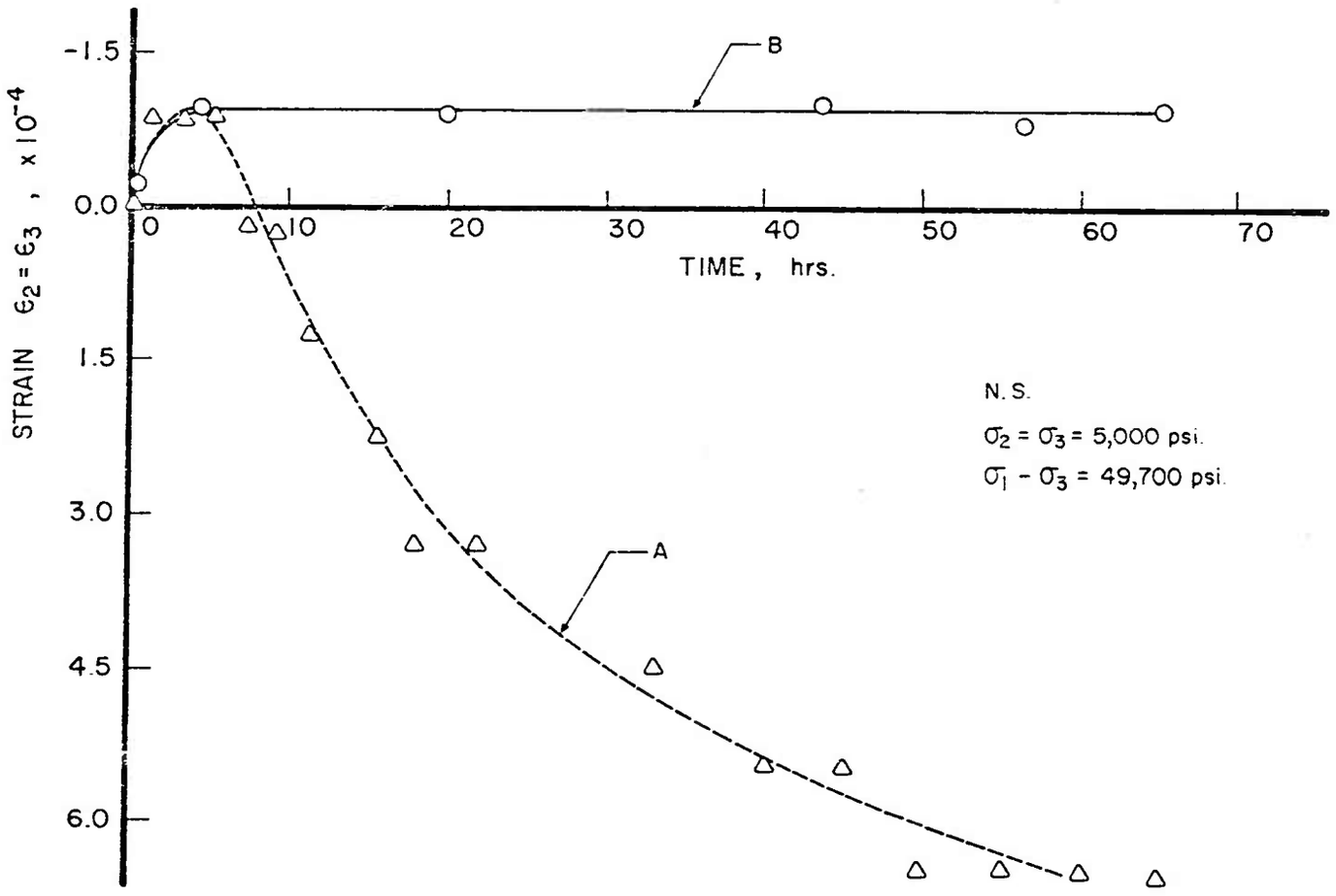

FIGURE 17. Creep Curves ϵ_3 Versus Time for Water-Saturated Nugget Sandstone at $\sigma_1 - \sigma_3$ = 49,700 psi (343 MN/m^2) and 5,000 psi (34.5 MN/m^2) Confining Pressure. Stress Histories prior to Deviatoric Loading: Sample A - 5,000 psi (34.5 MN/m^2) Hydrostatic Pressure for 16 hours; Sample B - 5,000 psi (34.5 MN/m^2) Hydrostatic Pressure for 72 Hours.

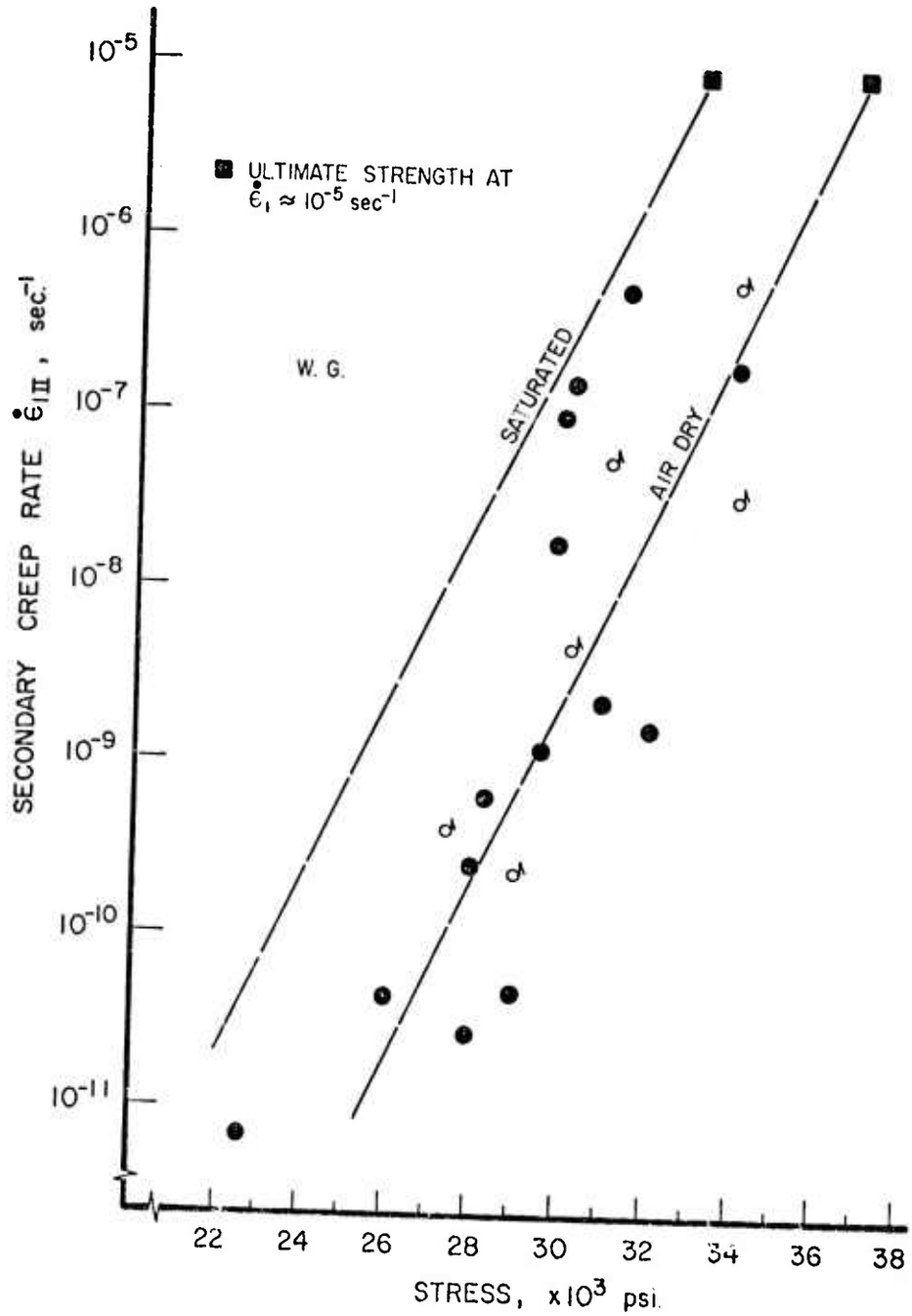

FIGURE 18. Secondary Creep Rate $\dot{\epsilon}_{II}$ versus Stress for Air-Dry Westerly Granite in Uniaxial Compression (Semi-Logartihmic Representation).

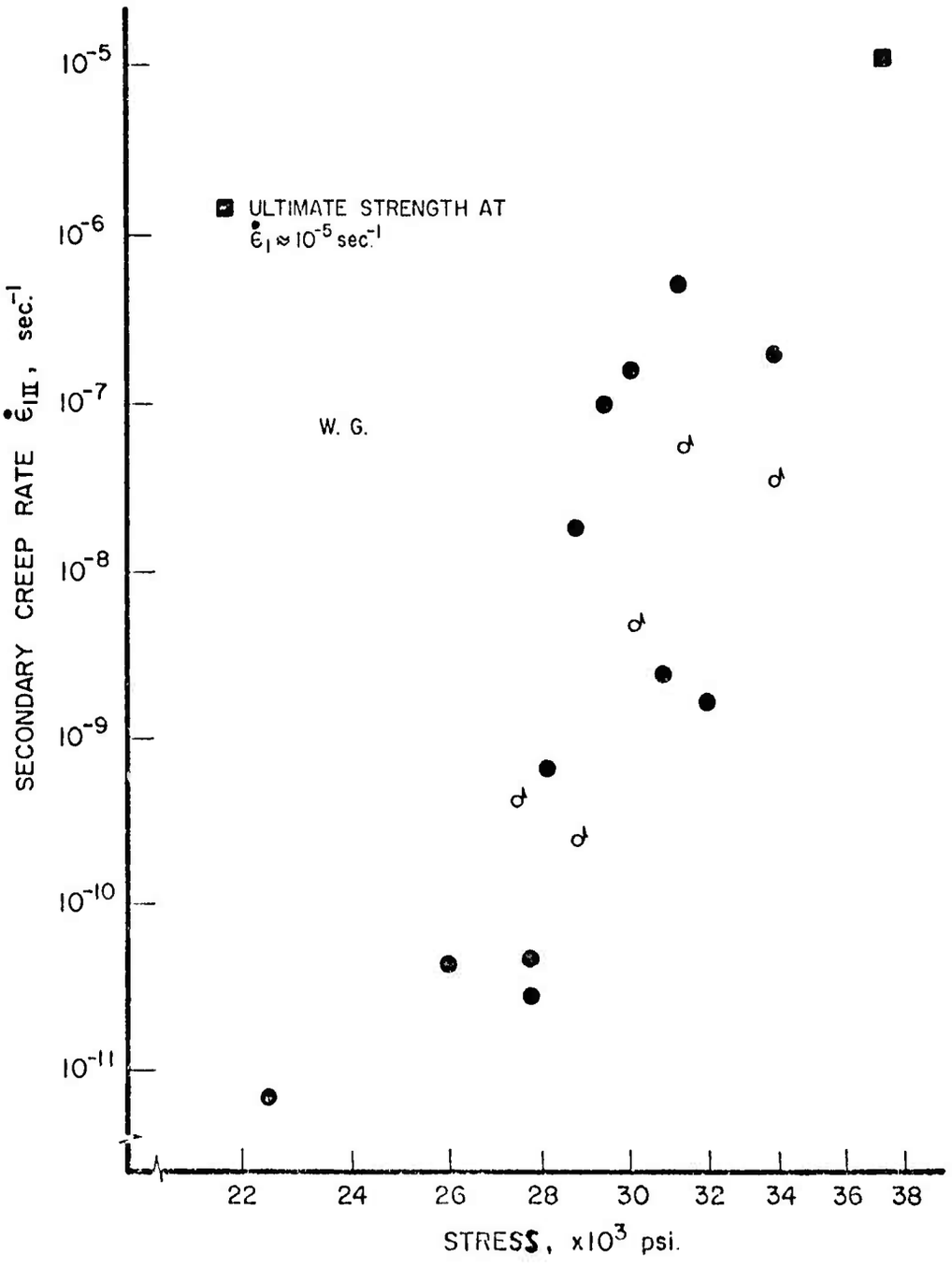

FIGURE 19. Secondary Creep Rate $\dot{\epsilon}_{III}$ versus Stress for Air-Dry Westerly Granite in Uniaxial Compression (Double-Logarithmic Representation).

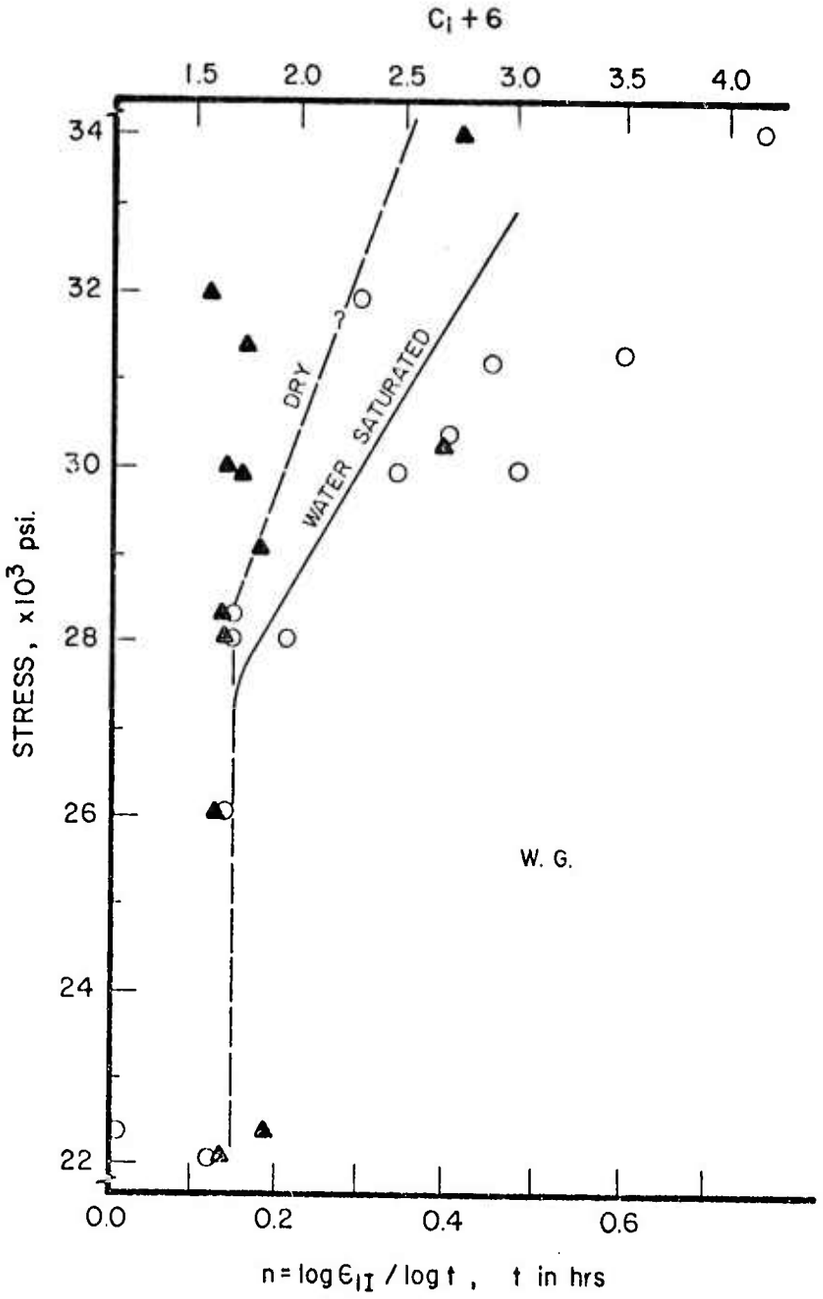

FIGURE 20. Some Parimary Creep Data for Air-Dry Westerly Granite in Uniaxial Compression Assuming $\varepsilon_{iI} = 10^{C_i} t^{n_i}$; values of C_1: Closed Triangles; Values of n_1: Open Circles.

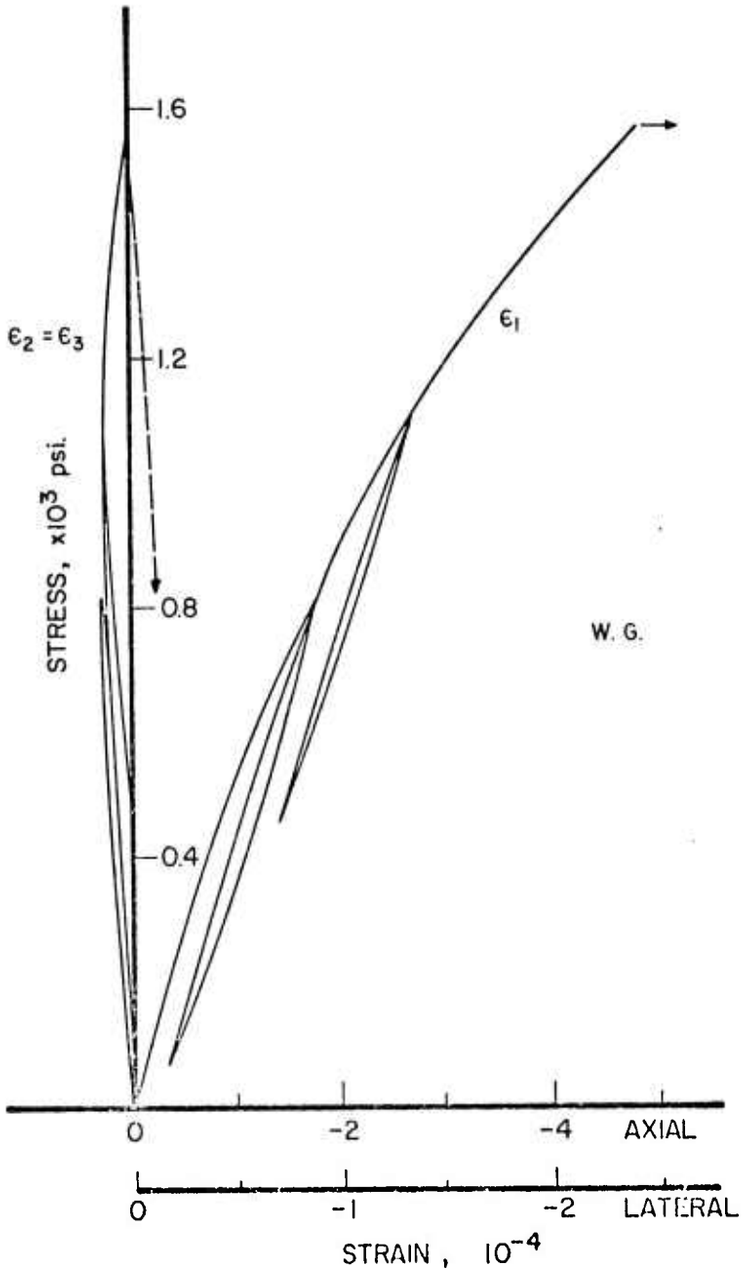

FIGURE 21. Typical Quasi-Static Stress-Strain Curves for Air-Dry Westerly Granite in Uniaxial Tension (strain rate $\dot{\epsilon}_1 \approx$ 10-6/sec.

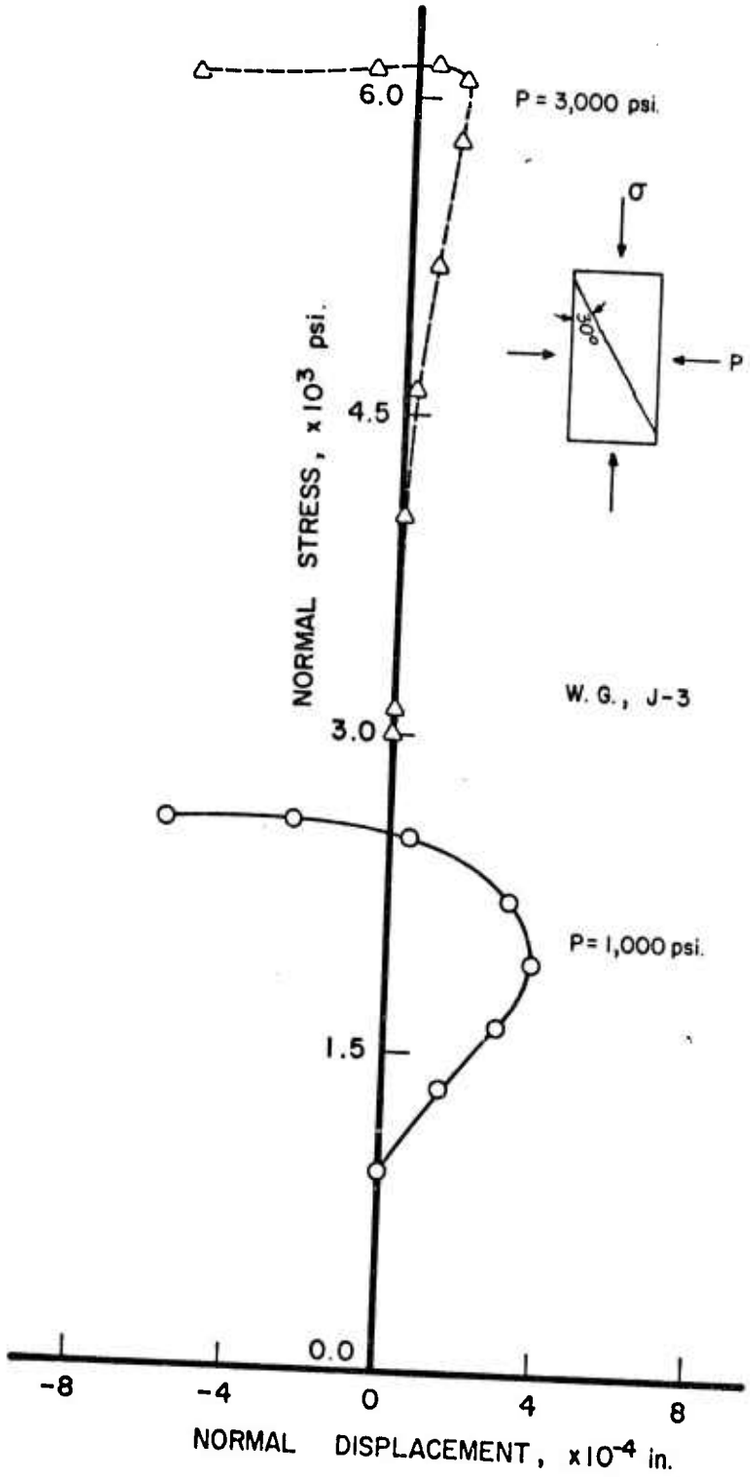

FIGURE 22. Average Normal Stress σ_n Versus Average Normal Displacement d_n for Rough Tension Joint in Water-Saturated Westerly Granite Cylinder in Quasi-Static Confining Pressure Experiments ($d_n > 0$ denotes Joint Closure).

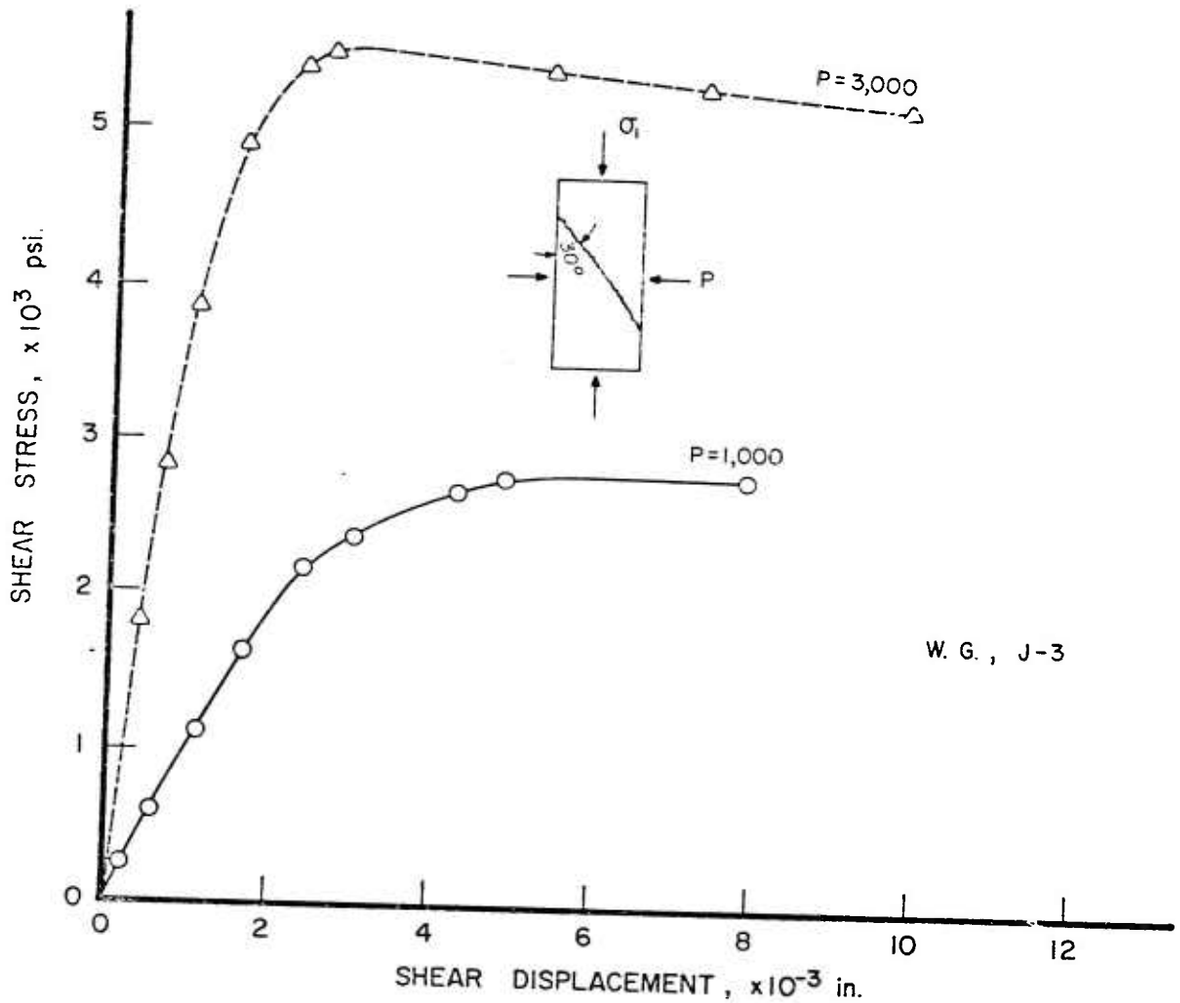

FIGURE 23. Average Shear Stress τ_n versus Average Shear Displacement d_s for Rough Tension Joint in Water-Saturated Westerly Granite Cylinder in Quasi-Static Confining Pressure Experiments.

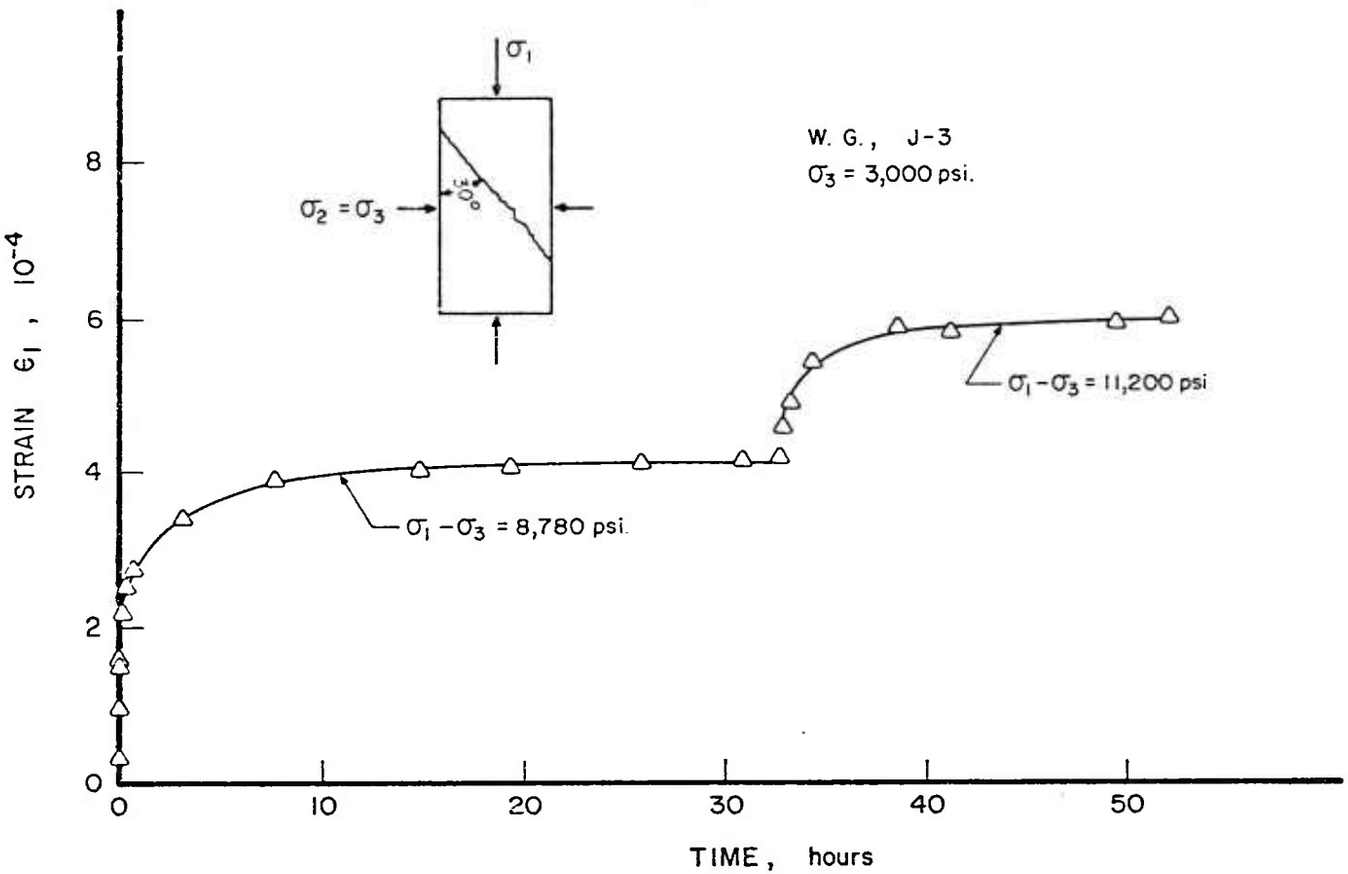

FIGURE 24. Axial Strain ε_1 Versus Time for Jointed, Water-Saturated Westerly Granite under Constant Deviatoric Shear Stress and Confining Pressure.

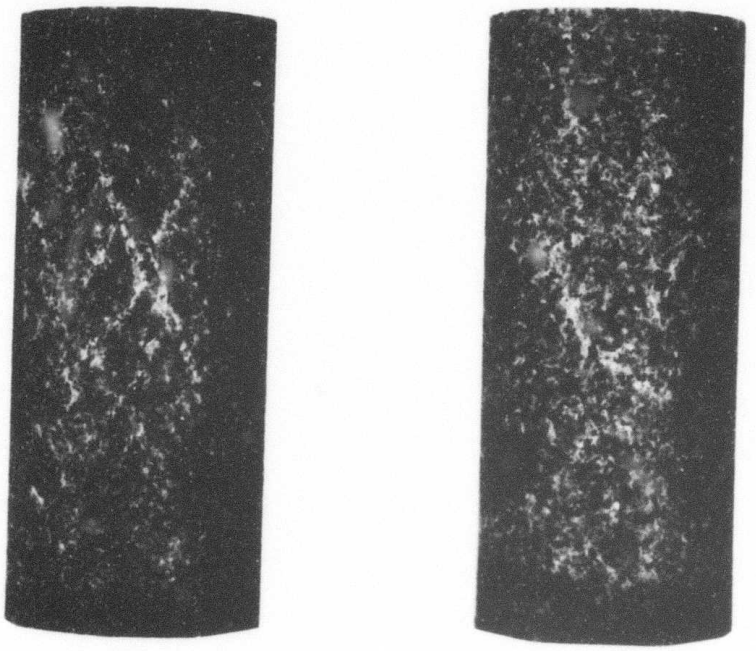

FIGURE 25. Visible Fracture Patterns in Water-Saturated Granite at 5,000 psi Confining Pressure. Loading Histories: (a) Quasi-Static Loading Just Beyond Ultimate Strength; (b) Constant Stress Difference $\sigma_1 - \sigma_3$ = 69,900 psi (96% of Ultimate Strength) for 375 Hours.

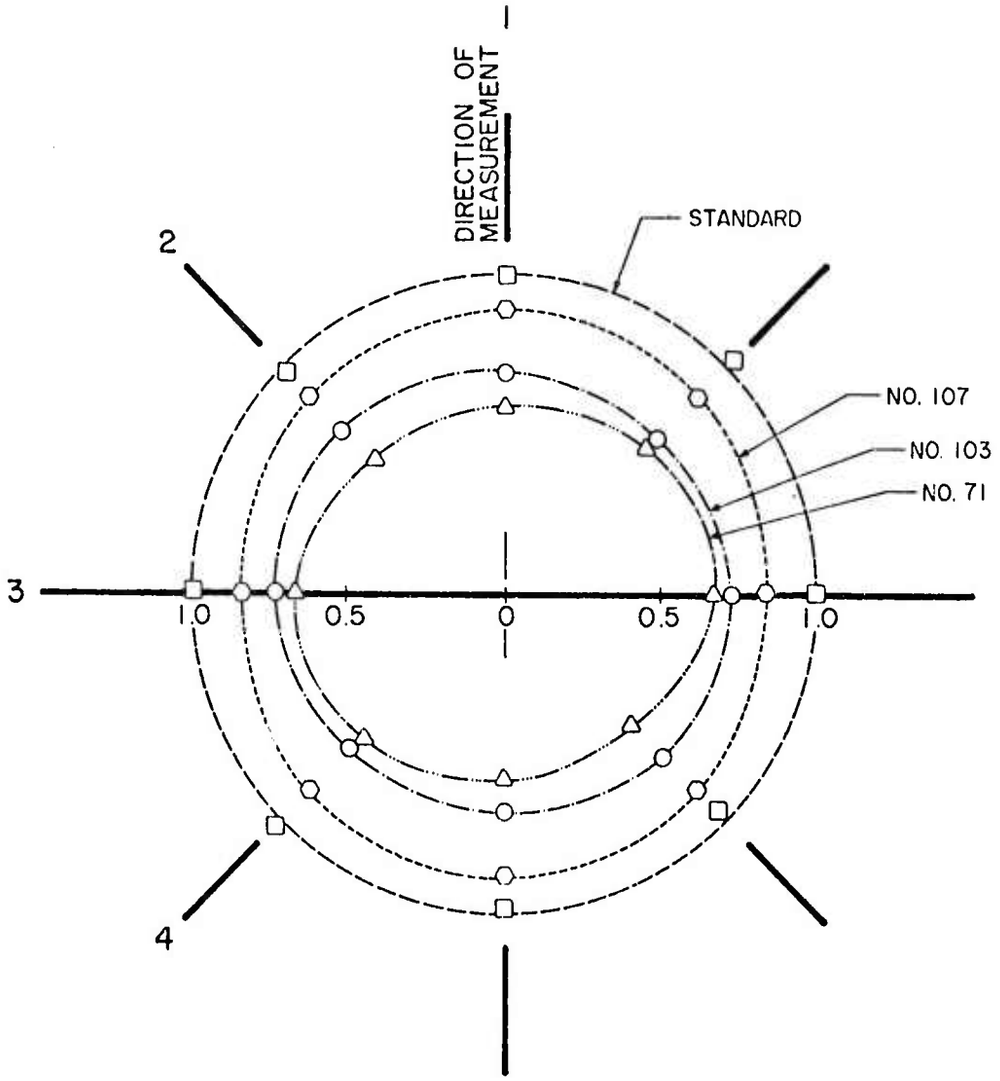

FIGURE 26. Polar Plot of Ultra-Sonic Velocities Perpendicular to σ_1 in Water-Saturated Westerly Granite at 5,000 psi Confining Pressure. Loading Histories: Sample 71, Quasi-Static Loading just beyond Ultimate Strength; Sample 107, Quasi-Static Loading just below Ultimate Strength; Sample 103, Constant Stress Difference $\sigma_1-\sigma_3$ = 69,900 psi (96% of ultimate strength) for 375 Hours. Velocities are Normalized with Respect to Average Undeformed, Standard Sample.

APPENDIX

References of Report, "Creep Fracture of Rock in Uniaxial Compression." ARPA Contract No. HO110054, 1971.

1. Michelson, A. A., "The Laws of Elastico-Viscous Flow," J. Geol., 47, 3, 1939.

2. Griggs, D. T., "Deformation of Rocks Under High Confining Pressure," J. Geol., 44, 5, 1936.

3. Griggs, D. T., "Creep of Rocks," J. Geol., 47, 3, 1939.

4. Phillips, D. W., "Tectonics of Mining," Colliery Eng., XXV, 1948.

5. Lomnitz, C., "Creep Measurements in Ignious Rocks," J. Geol., 64, 5, 1956.

6. Hardy, H. R., "Time Dependent Deformation and Failure of Geologic Materials," Colorado School of Mines, Quart., 54, 1959.

7. Robertson, E. G., "Creep of Solenhofen Limestone Under Moderate Hydrostatic Confining Pressure," Geol. Soc. Am. Mem., 79, 1960.

8. Matsushima, S., "On the Flow and Fracture of Rocks," Bull. Disast. Prev. Res., Inst., Kyoto Univ., 36, 1, 1960.

9. Robertson, E. G., "Viscoelasticity of Rocks," State of the Earth's Crust, Am. Elsencir Publ. Co., 1964.

10. Misra, A. K., and Murrell, S. A., "An Experimental Study of the Effect of Temperature and Stress on the Creep of Rocks," Geophys. J. R. Astr. Soc., 9, 509, 1965.

11. LeComte, P., "Creep in Rock Salt," J. Geol., 72, 469, 1965.

12. Dreyer, W., Die Festigkeitseigenschaften natuerlicher Gesteine, insbesondere der Salz- und Karbongesteine, Clausthaler Hefte, Heft 5, Verlag Gebrueder Borntraeger, Goslar, Germany, 1967.

13. Rummel, F., "Untersuchungen der zeitabhaengigen Verformung einiger Granit- und Eklogit-Gesteinsproben unter einachsiger konstanter Druckspannung und Temperaturen bis 400°C," PhD thesis, University of Munich, Germany, 1967.

14. Scholz, C. H. "Mechanism of Creep in Brittle Rock," J. Geophys., Res. 73, 10, 1968.

15. Cruden, D. M., "Creep Law for Rock Under Uniaxial Compression," Int. J. Rock Mech. Min. Sci., 8, 2, 1971.

16. Cruden, D. M. "Single Increment Creep Experiments on Rock Under Uniaxial Compression," ibid.

17. Heard, H. C., "The Effects of Large Changes of Strain Rate in the Experimental Deformation of Rock," J. Geol., 71, 2, 1963.

18. Simpson, D. R., and Fergus, J. H., "The Effect of Water on the Compressive Strength of Diabase,"

19. Krokosky, E. M. and Husak, A., "Strength Characteristics of Basalt-Like Rock in Ultra-High Vacuum," J. Geophys. Res., 73, 6, 1968.

20. Colback, P. S. B., and Wiid, B. L., "The Influence of Moisture Content on the Compressive Strength of Rock," Rock Mech. Symp. University of Toronto, 1965.

21. Scholz, C. H., personal communication, 1971

22. Martin, R. J. III, "Time Dependent Crack Growth in Quartz," Trans. Am. Geophys. Union, 52, 4, 1971.

23. Glathart, J. R., and Preston, F. W., "Fatigue Models in Glass," J. Appl. Phys, 17, 3, 1946.

24. Charles, R. J., "The Strength of Silicate Glasses and Some Crystalline Oxides," Proc Intern. Conf. on Fracture, MIT Press, 1959.

25. LeRoux, H., "The Strength of Fused Quartz in Water Vapor," Proc. Poy. Soc. London, A 286, 390, 1965.

26. Brace, W. F., and Martin, III, "A Test of the Law of Effective Stress for Crystalline Rocks of Low Porosity," Int. J. Rock Mech. Min. Sci., 5, 2, 1968.

27. Cornet, F. H., "The Effect of Pore Fluid on the Mechanical Behavior of Rocks," Proc. 13th Symp. Rock Mech., University of Illinois, 1971.

28. Serdengecti, S., and Boozer, G. D., "The Effect of Strain Rate and Temperature on the Behavior of Rocks Subjected to Triaxial Compression," Min. Ind. Exp. Sta. Bull., Penn. State Univ., 76, 1961.

29. Price, N. J., "A Study of Time-Strain Behavior in Coal Measure Rocks," Inv. J. Rock Mech. Min. Sci., 1, 2, 1964.

30. Green, S. J., and Perkins, R. D., "Uniaxial Compression Tests at Strain Rates from 10^{-4}/sec. to 10^{4}/sec on Three Geological Materials," General Motors Corp., Report MSL-68-6, 1968.

31. Baker, J., and Preston, F. W., "Fatigue of Glass Under Static Loads," J. Appl. Phys., 17, 1946.

32. Odqvrist, F. K. G., "On Theories of Creep Fracture," VIII Inv. Congr. Appl. Mech., Istanbul, 1962.

33. Bieniawski, T. Z., "Mechanism of Brittle Fracture of Rock," Int. J. Rock Mech. Min. Sci., 4, 4, 1967.

34. Brace, W. F. Paulding, B. W., and Scholz, C. H., "Dilantancy in the Fracture of Crystalline Rocks," J. Geophys. Res., 71, 16, 1966.

35. Mogi, K., "Study of Elastic Shocks Caused by the Fracture of Heterogeneous Material and its Relation to Earthquake Phenomena," Bull. Earthquake Res. Instit., Tokyo University, 40, 1962.

36. Duvall, W. I., and Obert, L., "Microseismic Method of Predicting Rock Failure in Underground Mining," U. S. Bur. Mines, Dept. Inv. 3797, 1942.

37. Scholz, C. H., "Microfracturing and the Inelastic Deformation of Rock in Compression," J. Geophys., 73, 4, 1968.

38. Wawersik. W. R., "A Study of Brittle Rock Fracture in Laboratory Compression Experiments," Int. J. Rock Mech. Min. Sci., 7, 4, 1970.

39. Wawersik, W. R., and Brace, W. F., "Post-Failure Behavior of a Granite and Diabase," Rock Mech., 3, 3, 1971.

40. Hult, J., Creep in Engineering Structures, Blaisdell Publ. Co., 1966.

41. Mendelson, A., "Plasticity: Theory and Applications, MacMillan Co., 1968.

42. Conrad, H., "Experimental Evaluation of Creep and Stress Rupture," Mech. Behavior at Elevated Temperatures, J. E. Dorn, ed., McGraw-Hill, 1961.

43. Baer, E., ed., Engineering Design for Plastics, Reinhold Book Co., 1964.

44. Fitzgerald, J. E., and Hufferd, W. L., Handbook for the Engineering Structural Analysis of Solid Propellants, in press.

45. Bland, D. R., The Theory of Linear Viscoelasticity, Pergamon Press, 1960.

46. Nadai, A., Theory of Fracture and Flow of Solids, Vol. 2, McGraw-Hill, 1963.

47. Flügge, W., Viscoelasticity, Blaisdell Publ. Co., 1967.

48. Ferry, J. D., Viscoelastic Properties of Polymers, John Wiley and Sons, Inc., 1970.

49. Christensen, R. M., Theory of Viscoelasticity, Academic Press, 1971.

50. Goetze, C., "High Temperature Rheology of Westerly Granite," J. Geophys. Res., 76, 5, 1971.

51. Brady, B. T., "A Mechanical Equation of State for Brittle Rock. Part I - The Pre-Failure Behavior of Brittle Rock," Int. J. Rock Mech. Min. Sci., 7, 4, 1970.

52. Smith, T. L., "Ultimate Tensile Properties of Elastomers. I. Characterization by a Time and Temperature Independent Failure Envelope," J. Polymer Sci., Part A, 1, 12, 1963.

53. Brace, W. F., "Brittle Fracture of Rocks," State of the Earth's Crust, W. R. Judd, ed., Am. Elsencir Publ. Co., 1964.

54. Brown, W. S. and Swanson, S. R., "Stress-Strain and Fracture Properties of Nugget Sandstone," UTEC ME 71-058, University of Utah, 1971.

55. Seldenrath, T. R. and Gramberg, J., "Stress-Strain Relations and Breakage of Rock," Mechanical Properties of Non-Metallic Brittle Materials, W. H. Walton, ed., Buttersworth Sci. Publ. Co., 1958.

56. Wawersik, W. R., "Detailed Analysis of Rock Failure in Laboratory Compression Tests," Ph.D. Thesis, University of Minnesota, 1968.

57. Pincus, H. J., "Optical Processing of Rectorial Rock Fabric Data," Proc. First Congr. Int. Soc. Rock. Mech., Lisbon, 1966.